AEROSPACE RESEARCH • AERODYNAMICS • PROPULSION • STRUCTURAL DYNAMICS • ELECTRONIC SYSTEMS AND INSTRUMENTS • COMPUTER MODULES

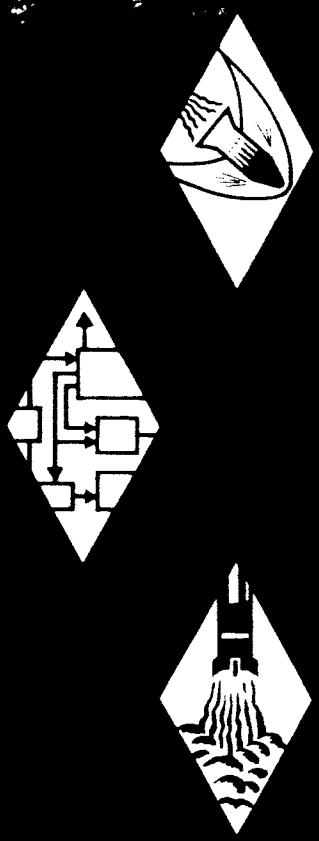

RESEARCH
ENGINEERING
PRODUCTION

TECHNICAL REPORT NO. 332

SLOT INJECTION OF REACTIVE GASES IN LAMINAR FLOW WITH APPLICATION TO HYDROGEN DUMPING

by Paul A. Taub

GENERAL APPLIED SCIENCE LABORATORIES, INC.
MERRICK and STEWART AVENUES, WESTBURY, L.I., N.Y. · (516) ED 3-6960

Dft 31048

Job 5487

Total No. Pages - ii and 60

Copy No. (15) of 16

TECHNICAL REPORT No. 332

SLOT INJECTION OF REACTIVE GASES IN LAMINAR FLOW WITH APPLICATION TO HYDROGEN DUMPING

By Paul A. Taub

Prepared for

GEORGE C. MARSHALL SPACE FLIGHT CENTER
HUNTSVILLE, ALABAMA
Under Contract No. NAS8-2686

Prepared by

Research Department
GENERAL APPLIED SCIENCE LABORATORIES, INC.
Merrick and Stewart Avenues
Westbury, L. I., New York

January 2, 1963

Approved by: Antonio Ferri
President

TABLE OF CONTENTS

TECHNICAL REPORT No 332

SLOT INJECTION OF REACTIVE GASES IN LAMINAR FLOW WITH APPLICATION TO HYDROGEN DUMPING

By Paul A. Taub

33867

ABSTRACT

The slot injection of reactive gases into a high speed airstream has been investigated. The chemical and transport properties have been simplified and calculations have been carried out for the case of a prescribed constant wall temperature.

Computations for hydrogen injection into an airstream flowing over a flat plate are presented and compared with the related, but more restricted theory of Libby and Schetz.

Results illustrate the advantages of injecting cold gases into the boundary layers of launch vehicles. In many cases, reactions may be assumed to occur; then, it is seen that the heat transfer rise associated with combustion may be delayed for substantial distances downstream from a slot injector and occurs in a region of relatively low heat transfer.

INTRODUCTION

During the boost phase of a missile flight, chemically reactive gases may be dumped overboard from the upper stages of the vehicle. Combustion of these gases with the high speed airstream can lead to critical heating and alterations of the forces and moments influencing the vehicle.

A series of studies intended to permit evaluation of the effects of gas discharges is being carried out. In Ref. 1 the available ignition delay characteristics associated with the induction time of hydrogen air mixtures were applied to a typical launch trajectory in order to estimate the minimum flow lengths according to the chemical kinetics of such mixtures. It was found that minimum lengths occur at altitudes of about 150,000 feet, where the flight velocity is about 6,000 ft/sec. At lower altitudes, the static temperatures in the neighborhood of the vehicle are relatively low, while at higher altitudes, the static pressures are low; lengths required for heat release are considerably larger at altitudes other than that yielding the minimum length.

The present study is concerned with the injection of gaseous hydrogen from a slot. The flow properties and configuration have been highly idealized in order to make the analysis tractable; the configuration is shown schematically in Fig. 1. The flow is assumed to be laminar, with simple transport properties, (i.e. unit Prandtl and Lewis numbers) and with the gases in chemical equilibrium so that the rates are controlled by mixing. The wall temperature is taken to be constant although this assumption complicates the analysis.

Libby and Schetz (Ref. 2) have provided an analysis of the problem based on satisfaction of the integral boundary layer equations with profiles of velocity, total enthalpy and element mass fractions generated by solutions of the related Carrier-Oseen flow. As in many integral methods, there arise restrictions on the applicability of the analysis associated with the assumed profiles. In this case, the velocity ratio u_j/u_e is restricted to the range $\frac{1}{3} < \frac{u_j}{u_e} < 1$. An additional, more complex restriction related to the enthalpies also prevails; it will be described below.

In the present report, the analysis of Ref. 2 is revised so as to remove the aforementioned restrictions. The solutions to the related flow are employed here, but the coordinate stretching, which in Ref. 2 was based on satisfying the complete equations on the average, is herein determined by satisfying the complete equations along a line within the boundary layer. Such a technique corresponds to collocation.

In the next section, the analysis extended by collocation is reviewed and compared with the relevent sections of Ref. 2. Subsequently, it is employed to show the effect of equilibrium chemical behavior on heat transfer to the surface of the vehicle under conditions consistent with the basic assumptions of the analysis.

The author is pleased to acknowledge the helpful suggestions of Dr. Paul A. Libby, Dr. Joseph A. Schetz, and the help of Mrs. Leatrice Groffman in carrying out the numerical computations.

ANALYSIS

As shown in Fig. (1), the system studied is that of hydrogen injected into an airstream by means of a wall slot. The boundary layer approximations are applied; the flow is of the non-similar type associated with the initial value problem of boundary layer theory. In the following analysis, the idealizations of laminar, steady and constant pressure flow will be applied. The influence of boundary layers on the wall (y= o) and on the splitter plate (y= a) for x<o is neglected; thus the initial velocity, composition and total enthalpy profiles are taken as step functions. For simplicity, the chemical behavior is taken to correspond to frozen flow and to the flame sheet approximation to equilibrium flow (cf, eg. Ref. 3). The frequently employed assumptions that the Prandtl number and all Lewis numbers are unity, are used. The $\rho\ \mu$ product, denoted C when non-dimensionalized with respect to $\rho_e \mu_e$ is taken to be, at most, a function of a streamwise coordinate χ.

The equations of motion are transformed by a combined Howarth-Dorodnitsyn and Mangler method.

eg:

$$\tau = \frac{\int_o^y \frac{\rho}{\rho_e}\, dy'}{\frac{\rho_j}{\rho_e}\, a} \quad , \quad \xi = \frac{r^{-k} \int_o^x r^{2k}\, dx'}{\frac{\rho_j}{\rho_e}\, a} \qquad (1)$$

$$\hat{u} = u/u_e \quad , \quad \hat{v} = v^*/u_e$$

$$v^* = r^{-k} \frac{\rho}{\rho_e} \left[v - u \left(\frac{\partial y}{\partial x} \right)_\tau \right]$$

where k= o and 1 for two-dimensional and axisymmetrical flow, respectively.

As in the method of Ref. 2, approximate solutions are generated in the spirit of the Carrier-Lewis modified Oseen method, by linearizing the convective operator in the transformed equations to be:

$$\hat{u}\,\frac{\partial}{\partial \xi} + \hat{v}\,\frac{\partial}{\partial \tau} \approx \hat{u}'\,\frac{\partial}{\partial \xi}$$

where $\hat{u}'$ is the effective connective velocity and is an, as yet, undetermined function of ξ (or χ) and may be a different function of ξ for the momentum equation than for the species conservation equations or the energy equation. The velocity $\hat{u}'$, for a particular equation, is determined here by satisfying the exact equation along a line in the flow with the solution found from the corresponding linearized equation.

I: VELOCITY DISTRIBUTION

As a consequence of the above assumptions, the velocity field in the (ξ,τ) plane may be determined before solution of the energy and species conservation equations.

The continuity and momentum equations form a system of equations and boundary conditions:

$$\frac{\partial \hat{u}}{\partial \xi} + \frac{\partial \hat{v}}{\partial \tau} = 0$$

$$\hat{u}\,\frac{\partial \hat{u}}{\partial \xi} + \hat{v}\,\frac{\partial \hat{u}}{\partial \tau} = \frac{1}{\rho_e \mu_e}\,\frac{\partial}{\partial \tau}\left(\frac{C\mu_e}{\eta_a}\,\frac{\partial \hat{u}}{\partial \tau}\right) \qquad (2)$$

$$\hat{u}(\xi,o) = \hat{v}(\xi,o) = 0, \quad \hat{u}(\rho,\infty) = 1$$

$$\hat{u}(o,\tau) = \begin{cases} \hat{u}_j & ; \quad o < \tau \leq 1 \\ 1 & ; \quad \tau > 1 \end{cases}$$

where

$$C = \frac{\rho \mu}{\rho_e \mu_e}, \qquad \eta_a = r^k \frac{\rho_j}{\rho_e}\, a$$

Using the linearization in the momentum equation and applying the transformation

$$\frac{dS}{d\xi} = \frac{C u_e}{\rho_e u_e \eta_a \hat{u}'} \qquad (3)$$

Reduces the momentum equation to

$$\frac{\partial \hat{u}}{\partial S} = \frac{\partial^2 \hat{u}}{\partial \tau^2} \qquad \tau = o : \hat{u} = o, \quad \tau \to \infty : \hat{u} = 1$$
$$S = o : \hat{u} = \begin{cases} \hat{u}_j & ; \quad o < \tau \leq 1 \\ 1 & \quad \tau > 1 \end{cases} \qquad (4)$$

This corresponds to the one-dimensional, semi-infinite heat conduction problem with initial temperature distribution given as a step function about S= 1.

The solution is well known in heat conduction theory (cf Ref. 4), and is:

$$\hat{u} = \hat{u}_j \ \text{erf}\left(\frac{\tau}{\sqrt{4S}}\right) + \frac{1-\hat{u}_j}{2}\left[\text{erf}\left(\frac{\tau-1}{\sqrt{4S}}\right) + \text{erf}\left(\frac{\tau+1}{\sqrt{4S}}\right)\right] \qquad (5)$$

The coordinate transformation is as yet undetermined; that is, the effective velocity of convection, $\hat{u}'(S)$ is unknown a priori. Libby and Schetz (2) determine $\hat{u}'$ (or equivalently, $\frac{dS}{d\xi}$) by satisfying the momentum integral equation at every station along the wall. This satisfied the momentum equation in the slot flow on the average and gives rise to an algebraic equation for $\hat{u}'$ or a relation for the variable $\frac{\mu_e C}{\rho_e u_e \eta_a}\xi$ as a function of S which reduces to a quadrature, (eg. Eq. (8) of Ref. 2). No restrictions are encountered.

In the present method, the exact differential equations are satisfied along a line in the flow; that is, $\frac{\tau}{\sqrt{4S}} = t = t\ (S)$. The procedure is as follows:

The exact equations (2) are written in the transformed S, τ coordinates as:

$$\frac{C\mu_e}{\rho_e u_e \eta_a \hat{u}'}\frac{\partial \hat{u}}{\partial S} + \frac{\partial \hat{v}}{\partial \tau} = 0, \quad \frac{C_{\mu_e}}{\rho_e u_e \eta_a \hat{u}'}\hat{u}\frac{\partial \hat{u}}{\partial S} + \hat{v}\frac{\partial \hat{u}}{\partial \tau} = \frac{C_{\mu_e}}{\rho_e u_e \eta_a}\frac{\partial^2 \hat{u}}{\partial \tau^2} \qquad (6)$$

From the continuity equation

$$\hat{v} = \frac{C_{\mu_e}}{\rho_e u_e \eta_a \hat{u}'}\left[\int_0^\tau \frac{\partial \hat{u}}{\partial S}\, d\tau\right] = \frac{C_{\mu_e}}{\rho_e u_e \eta_a \hat{u}'}\left[\left(\frac{\partial \hat{u}}{\partial \tau}\right)_w - \frac{\partial \hat{u}}{\partial \tau}\right] \qquad (7)$$

Since $\hat{u}$ satisfies the equation:

$$\frac{\partial \hat{u}}{\partial S} = \frac{\partial^2 \hat{u}}{\partial \tau^2}$$

The momentum equation (6) at a point of collocation, is reduced to a relation for $\hat{u}'$

$$\left[\left(\frac{\partial \hat{u}}{\partial \tau}\right)_w - \frac{\partial \hat{u}}{\partial \tau}\right] \frac{\partial \hat{u}}{\partial \tau} = (\hat{u}' - \hat{u}) \frac{\partial^2 \hat{u}}{\partial \tau^2} \qquad (8)$$

By appropriately choosing the collocation points (i.e. $t(S)$), $\hat{u}'$, is determined uniquely as a function of S. The choice of such points is discussed separately in Section VI. Note, however, that $\frac{\partial^2 \hat{u}}{\partial \tau^2}$ must never be allowed to equal zero at a collocation point.

Assuming that C is expressed in terms of S, then the inversion of the coordinate transformation may be expressed as:

$$\chi = a R_{e_a} \left(\frac{\rho_j}{\rho_e}\right)^2 \int_o^S \frac{\hat{u}'}{C} \, dS \qquad (9)$$

where

$$R_{e_a} = \frac{\rho_e u_e a}{\mu_e}$$

Thus, if C is taken as a constant, $\frac{\chi}{a} \frac{C}{R_{e_a}} \left|\frac{\rho_j}{\rho_e}\right|^2 = \frac{\chi}{\eta_a}\left|\frac{\mu_e C}{\rho_e u_e \eta_a}\right|$ can be obtained as a function of S with $\hat{u}_j$ as the sole parameter. This function is not shown herein; in general, C is not taken constant here, being evaluated at the wall.

II. SKIN FRICTION

The general expression for the skin friction coefficient is of interest. Thus,

$$\tau_w = \mu_w \left(\frac{\partial u}{\partial y}\right)_w = \mu_w \mu_e \left(\frac{\partial \hat{u}}{\partial \tau}\right)_w \frac{\partial \tau}{\partial \eta} \frac{\partial \eta}{\partial y} = \frac{\mu_e \mu_e C r^k}{\eta_a} \left(\frac{\partial \hat{u}}{\partial \tau}\right)_w$$

$$C_f = \frac{\tau_w}{\rho_e u_e^2} = \frac{\mu_e C r^k}{\rho_e u_e \eta_a} \left(\frac{\partial \hat{u}}{\partial \tau}\right)_w \tag{10}$$

and

$$\frac{\rho_e u_e \eta_a}{\mu_e C} r^{-k} C_f = (\pi S)^{-1/2} \left[\hat{u}_j + (1-\hat{u}_j) \exp\left(-\frac{1}{4S}\right)\right]$$

A. Comparison With Flat Plate (No Slot)

The case of $\hat{u}_j = 1$ is of interest, since this analysis then corresponds to an approximate solution of the flat plate boundary layer problem; the solution is given in terms of the similarity variable $t = \frac{\tau}{\sqrt{4S}}$ and collocation amounts to satisfying the exact equation (2) at a particular value of t; thus $\hat{u}'$ is a constant.

For k=o or constant r and $C = \frac{\rho_w u_w}{\rho_e \mu_e} = 1$

$$\left(\frac{\rho_e u_e \chi}{\mu_e}\right)^{1/2} C_f = \left(\frac{\hat{u}'}{\pi}\right)^{1/2} \tag{11}$$

With no slot, the flow is similar in t, and collocation is required at only one specific value of the independent variable (cf Ref. 3).

To recover the Blasius result for the flat plate without injection, one must have $\hat{u}' = 0.346$. This corresponds to collocating the solution at $t \cong 0.7$; if one collocates at length $t = 0.7$, it is found that $\hat{u}' = 0.363$ and that the skin friction is in error by $\approx 3\%$. The boundary layer edge corresponding to $\hat{u} = \frac{u}{u_e} = .99$ is found at $t \approx 2$.

B. Constant ρ μ Ratio

It is seen that for C taken to be constant, the distribution of $\frac{\rho_e u_e \eta_a}{\mu_e C} r^{-k} C_f = \frac{Re_a}{C}\left(\frac{\rho_j}{\rho}\right) C_f$ with $\left(\frac{\chi}{a}\right)' \frac{C}{Re_a}\left(\frac{\rho_j}{\rho_e}\right)^2$ may be obtained with $\hat{u}_j$ as a parameter. This permits a straightforward comparison of the skin friction distributions obtained by the method of Ref. 2 (cf Fig. 3). It will be noted that, in general, the agreement is satisfactory and that both approximate methods yield reasonable results.

III. COMPOSITION AND STATE DISTRIBUTIONS

It is convenient to consider next the solution for the distributions of the specie mass fractions; this solution requires a specification of the chemical system. In the present report, the external stream will be considered to be air containing oxygen and nitrogen,and the gas injected from the slot will be molecular hydrogen. For conditions of interest in a vehicle launch, the temperatures will be such that no significant dissociation of nitrogen will occur; thus nitrogen can be treated as an inert diluent. In addition, only equilibrium or frozen chemical behavior will be considered here; it is sufficient to consider water as the only product of combustion. As a further assumption, the equilibrium chemical behavior will be approximated by the so-called flame sheet model as outlined below.

The specie conservation equations under the assumptions of unity Prandtl and Lewis numbers may be written for the mass fraction of the i^{th} component as:

$$\hat{u}\frac{\partial Y_i}{\partial \xi} + \hat{v}\frac{\partial Y_i}{\partial \tau} = \frac{1}{\rho_e u_e}\frac{\partial}{\partial \tau}\left(\frac{C u_e}{\eta_a}\frac{\partial Y_i}{\partial \tau}\right) + r^{-2k}\frac{\eta_a}{\rho}\dot{w}_i \qquad (12)$$

with the boundary conditions:

$\tau = 0$: $\quad \dfrac{\partial Y_i}{\partial \tau} = 0$

$\tau \to \infty$: $\quad Y_i = Y_{i_e}$

$\xi = 0$: $\quad Y_i = Y_{i_j} \quad ; 0 < \tau \leq 1$

$\qquad\quad Y_i = Y_{i_e} \quad ; \tau > 1$

A. Chemistry

The reaction may be represented by

$$a_1 O_2 + a_2 H_2 + 3.76\ N_2 \rightarrow b_1 O_2 + b_2 H_2 + b_3 H_2O + 3.76\ N_2 \qquad (13)$$

The subscripts 1, 2, 3, 4 refer to O_2, H_2, H_2O, and N_2 respectively.

For unity Lewis numbers the introduction of the element mass fractions will eliminate the production terms in the specie continuity equations for O_2, H_2 and N_2. The element mass fractions are

$$\tilde{Y} \equiv Y_1 + \frac{W_1}{2W_3} Y_3 , \quad \tilde{Y}_2 \equiv Y_2 + \frac{W_2}{W_3} Y_3 , \quad \tilde{Y}_4 \equiv Y_4 \qquad (14)$$

and are suggested by the conditions of element conservation:

$$\dot{w}_1 + \frac{W_1}{2W_3} \dot{w}_3 = 0 , \quad \dot{w}_2 + \frac{W_2}{W_3} \dot{w}_3 = 0, \quad \dot{w}_4 = 0$$

Either the equilibrium condition (law of mass action) or the statement $Y_3 = 0$ (frozen condition) completes the set of equations defining the composition. For the temperatures of interest here, the equilibrium constants are large implying small mass fractions for either oxygen or hydrogen. This, in addition to the slot geometry, suggests utilization of a flame sheet model. At the flame sheet: $Y_1 = Y_2 = 0$ and from the definitions of Y_1 and Y_2:

$$\frac{2}{W_1} Y_{1_f} = \frac{Y_{2_f}}{W_2} \qquad (15)$$

Since $\tilde{Y}_1$ and $\tilde{Y}_2$ are functions of ξ and τ this equation defines a relation between the independent variables which specifies the flame sheet shape.

For the slot problem under discussion the hydrogen is completely consumed when the flame sheet reaches the wall, (i.e. $\tau_f = 0$ at $\xi = \xi^*$). The flame sheet divides the region into two parts, termed I and II, in which $Y_1 = 0$ and $Y_2 = 0$, respectively. Thus region I extends from the wall ($\tau = 0$) to the flame, as long as $\tau \geq 0$; region II extends from the flame sheet outwards to $\tau \to \infty$ and from the wall outwards when $\xi > \xi^*$. At the wall then, for ξ; $0 \leq \xi \leq \xi^*$, $Y_{1_w} = 0$ and for $\xi > \xi^*$, $Y_{2_w} = 0$. Hence, in terms of the element mass fractions, the specie continuity equation and boundary conditions are:

$$\hat{u}\frac{\partial \tilde{Y}_i}{\partial \xi} + \hat{v}\frac{\partial \tilde{Y}_i}{\partial \tau} = \frac{1}{\rho_e u_e}\frac{\partial}{\partial \tau}\left(\frac{C\mu_e}{\eta_a}\frac{\partial \tilde{Y}_i}{\partial \tau}\right) \quad \begin{matrix} i = 1,2,4 \text{ Flame Sheet} \\ i = 1,2,3,4 \text{ Frozen} \end{matrix}$$

$$\tau = 0 \quad \frac{\partial \tilde{Y}_i}{\partial \tau} = 0 \qquad \xi = 0 : \quad \tilde{Y}_i = \begin{cases} \tilde{Y}_{i_j} = Y_{i_j}\,; & 0 < \tau \leq 1 \\ \tilde{Y}_{i_e} = Y_{i_e}; & \tau > 1 \end{cases} \qquad (16)$$

$$\tau \to \infty \quad \tilde{Y}_i = \tilde{Y}_{i_e} = Y_{i_e}$$

B. Solution for the Element Mass Fractions

As in the solution for the velocity, the convective operator is now linearized. Thus, the i^{th} element conservation and continuity equation is

$$\hat{u}\frac{\partial \tilde{Y}_i}{\partial \xi} + \hat{v}\frac{\partial \tilde{Y}_i}{\partial \tau} \approx \hat{u}'\frac{\partial \tilde{Y}_i}{\partial \xi} = \frac{1}{\rho_e u_e}\frac{\partial}{\partial \tau}\left(\frac{C\mu_e}{\eta_a}\frac{\partial \tilde{Y}_i}{\partial \tau}\right) \qquad (17)$$

$$\frac{\partial \hat{u}}{\partial \xi} + \frac{\partial \hat{v}}{\partial \tau} = 0$$

with the appropriate boundary conditions.

The transformation:

$$\frac{dS_2}{d\xi} = \frac{C\mu_e}{\rho_e u_e \eta_a \hat{u}''} \quad ; \quad \hat{u}'' = \hat{u}''(S) \tag{18}$$

yields for the linearized energy equation:

$$\frac{\partial \tilde{Y}_i}{\partial S_2} = \frac{\partial^2 \tilde{Y}_i}{\partial \tau^2} \tag{19}$$

This corresponds to the unsteady heat conduction problem encountered in the solution for the velocity, but with different boundary conditions; the solution is

$$\tilde{Y}_i = \tilde{Y}_{i_e} + \frac{\tilde{Y}_{i_e} - \tilde{Y}_{i_j}}{2}\left[\operatorname{erf}\left(\frac{\tau - 1}{\sqrt{4S_2}}\right) - \operatorname{erf}\frac{\tau + 1}{\sqrt{4S_2}}\right] \tag{20}$$

This approximate solution may be compared with the exact equation and collocated along a line so as to relate S_2 to χ. As before

$$\frac{\partial \hat{v}}{\partial \tau} = -\frac{C\mu_e}{\rho_e u_e \eta_a \hat{u}''}\frac{dS}{dS_2}\frac{\partial^2 \hat{u}}{\partial \tau^2}$$

$$\frac{C\mu_e}{\rho_e u_e \eta_a \hat{u}''}\hat{u}\frac{\partial \tilde{Y}_i}{\partial S_2} + \hat{v}\frac{\partial \tilde{Y}_i}{\partial \tau} = \frac{C\mu_e}{\rho_e u_e \eta_a}\frac{\partial^2 \tilde{Y}_i}{\partial \tau^2} \tag{21}$$

Thus, the collocation condition is:

$$(\hat{u}'' - \hat{u})\frac{\partial^2 \tilde{Y}_i}{\partial \tau^2} = \frac{dS}{dS_2}\left[\frac{\partial \hat{u}}{\partial \tau}\right]_w - \frac{\partial \hat{u}}{\partial \tau}\frac{\partial \tilde{Y}_i}{\partial \tau} \tag{22}$$

where

$\frac{dS}{dS_2} = \frac{dS/d\xi}{dS_2/d\xi} = \frac{\hat{u}''}{\hat{u}'}$ is the ratio of the effective velocities of convection for the species conservation and momentum equations.

The forms of the $\widetilde{Y}_i$ solutions and the collocation condition show that $\hat{u}''$ is independent of the species conservation equation considered; that is, $\hat{u}''$ is independent of the index i. It is convenient to determine $\hat{u}''$ in terms of $\hat{u}'$ since in this formulation the, as yet, undetermined effective $\rho\,\mu$ (i.e. C) variation does not appear. Thus, only before the transformation into the physical plane, is it necessary to evaluate C e.g., as $\frac{\rho_w u_w}{\rho_e \mu_e}$; this allows the evaluation of C and the composition to be uncoupled.

In the method of Libby and Schetz (cf. p. 13 of Ref. 2), the condition for $\hat{u}''$ sets limits upon the jet velocity ratio u_j/u_e. They find, by requiring $\hat{u}''$ ($S_2 = o$) to be positive, then u_j must lie in the range $\frac{1}{3} \leq u_j/u_e < 1$.

C. Flame Sheet Location

As discussed above, the condition for locating the flame sheet is:

$$\frac{2}{W_1}\,\widetilde{Y}_{1_f} = \frac{\widetilde{Y}_{2_f}}{W_2} \tag{23}$$

The $\widetilde{Y}_1$ and $\widetilde{Y}_2$ solutions are obtained from equation (20) with appropriate values for $\widetilde{Y}_{i_e}$ and $\widetilde{Y}_{i_j}$ as

$$\widetilde{Y}_1 - Y_{1_e} = -\frac{Y_{1_e}}{2}\left[\operatorname{erf}\left(\frac{\tau+1}{\sqrt{4S_2}}\right) - \operatorname{erf}\left(\frac{\tau-1}{\sqrt{4S_2}}\right)\right]$$

$$\widetilde{Y}_2 = \frac{1}{2}\left[\operatorname{erf}\left(\frac{\tau+1}{\sqrt{4S_2}}\right) - \operatorname{erf}\left(\frac{\tau-1}{\sqrt{4S_2}}\right)\right] \tag{24}$$

so that the condition is

$$\frac{2W_2}{W_1}\,Y_{1_e}\,|1-\bar{X}| = Y_{2_j}\,\bar{X} \quad ; \quad \bar{X} = \frac{1}{2}\left[\operatorname{erf}\left(\frac{\tau_f+1}{\sqrt{4S_2}}\right) - \operatorname{erf}\left(\frac{\tau_f-1}{\sqrt{4S_2}}\right)\right] \tag{25}$$

Solution for $\bar{\chi}$ yields

$$\bar{\chi} = \frac{(2W_2Y_{1_e}/W_1)}{(2W_2Y_{1_e}/W_1) + Y_{2_j}} \tag{26}$$

Thus, $\tau_f(S_2)$ is determined. The point of impingement of the flame sheet on the body (i.e., $\tau_f = 0$ at $S_2 = S_2^*$) may be calculated by setting $\tau_f = 0$ and solving for S_2^*.

$$\text{erf}\left(\frac{1}{\sqrt{4S_2}}\right) = \frac{(2W_2Y_{1_e}/W_1)}{(2W_2Y_{1_e}/W_1) + Y_{2_j}} \tag{27}$$

In the slot problem:

$$Y_{1_e} = 0.232\,,\quad Y_{2_j} = 1\,,\quad W_1 = 32\,,\quad W_2 = 2$$

so that:

$$S_2^* = 406 \tag{28}$$

D. Wall Enthalpy: (Constant Wall Temperature)

It will be necessary for solution of the energy equation to have the distribution of wall enthalpy. For a constant wall temperature the above distributions of composition when applied to the wall permit the wall enthalpy to be computed as follows:

Equilibrium Chemistry:

$$0 \le S_2 \le S_2^* \;:\; h_{w_I}(S_2) = \frac{2}{W_1}(W_3h_{3_w} - W_2h_{2_w})\widetilde{Y}_{1_w} + h_{2_w}\widetilde{Y}_{2_w} + h_{4_w}Y_{4_w}$$

$$S_2 > S_2^* \;:\; h_{w_{II}}(S_2) = h_{1_w}\widehat{Y}_{1_w} + \frac{1}{W_2}\left(W_3h_{3_w} - \frac{W_1}{2}h_{1_w}\right)\widetilde{Y}_{2_w} + h_{4_w}Y_{4_w} \tag{29}$$

Frozen Chemistry:

$$h_{w_f}(S_2) = h_{1_w}\widehat{Y}_{1_w} + h_{2_w}\widetilde{Y}_{2_w} + h_{4_w}Y_{4_w}$$

$$= h_{1_w}Y_{1_w} + h_{2_w}Y_{2_w} + h_{4_w}Y_{4_w} \tag{30}$$

In general, the wall enthalpy may be represented by a function of the form

$$h_w = \gamma + 2\alpha\ \text{erf}\left(\frac{1}{\sqrt{4S_2}}\right)$$

IV. SOLUTION FOR THE ENERGY DISTRIBUTION

In order to determine the heat transfer and the flow in the physical, i.e., x, y plane, it is necessary to find the distribution of total enthalpy. As long as the distribution of h_w can be specified with X, S, S_2 (or S_3 as will be introduced below in connection with the approximate solution of the energy equation), it is possible to determine a coordinate stretch factor by the collocation technique.

The energy equation for unity Prandtl and Lewis numbers in terms of the total enthalpy is:

$$\hat{u}\,\frac{\partial h^\circ}{\partial \xi} + \hat{v}\,\frac{\partial h^\circ}{\partial \tau} = \frac{1}{\rho_e u_e}\,\frac{\partial}{\partial \tau}\left(\frac{C\mu_e}{\eta_a}\,\frac{\partial h^\circ}{\partial \tau}\right) \tag{31}$$

with

$\tau = 0$ $\qquad h^\circ = h_w$

$\tau \to \infty$ $\qquad h^\circ = h^\circ_e$

$\xi = 0$ $\qquad h^\circ = h^\circ_j;\ 0 < \tau \leq 1$

$\qquad\qquad h^\circ = h^\circ_e;\ \tau > 1$

A. Constant Wall Enthalpy Solution

Comparison of this system of equation and boundary conditions with the momentum equation and boundary conditions shows that a Crocco relation exists between the total enthalpy and the velocity fields if the wall enthalpy (h_w) is constant and if

$$h^\circ_j - h^\circ_e = (h_w - h^\circ_e)\,(1-\hat{u}_j) \tag{32}$$

The Crocco relation is

$$h^\circ - h^\circ_e = (h_w - h^\circ_e)\,(1-\hat{u}) \tag{33}$$

Thus, the enthalpy solution for constant h_w, is:

$$h^\circ = h - (h_w - h_j^\circ) \operatorname{erf} \frac{\tau}{\sqrt{4S}} + \frac{h_e^\circ - h_j^\circ}{2} \left[\operatorname{erf} \left(\frac{\tau - 1}{\sqrt{4S}} \right) + \operatorname{erf} \left(\frac{\tau + 1}{\sqrt{4S}} \right) \right] \quad (34)$$

Note that equation (32) implies a restriction among the flow parameters and thus that the solution given by equation (34) is applicable to flows compatible therewith.

B. Constant Wall Temperature Solution

An approximate solution for this case is obtained from the constant wall enthalpy solution by making a local similarity assumption as in Ref. 2. At any given ξ station, the total enthalpy profile is assumed to be that existing for a constant wall enthalpy solution with the same value of h_w. The given wall temperature and the solution for the element mass fractions determine the wall enthalpy distribution.

A better approximate solution would be found by solving the exact Rayleigh-Stokes problem associated with an arbitrary wall enthalpy distribution; this solution is shown in Appendix I. However, because of the simplicity of the approximate local similarity solution, it was used in the collocation procedure for the energy equation. Note that the collocation procedure will inherently compensate for this approximation.

The restriction associated with the constant wall enthalpy case does not apply, since the solution may be viewed as coming from the associated Rayleigh-Stokes problem - in which case, local collocation is performed.

Thus, the h° function (equation 34) is assumed to hold for the non-constant h_w boundary condition, in a system of coordinates (τ, S_3) which is related to the (τ, ξ) coordinate system by the transformation

$$\frac{dS_3}{d\xi} = \frac{C\mu_e}{\rho_e u_e \eta_a} \hat{u}''' \tag{35}$$

Substituting the h° function (equation 34) with τ & S_3 as the independent variables, into the exact energy equation (cf equation 31) and continuity equation, yields for the collocation condition, since h_w is not constant:

$$\frac{\hat{u}'''}{\hat{u}'}\left[\left(\frac{\partial \hat{u}}{\partial \tau}\right)_w - \frac{\partial \hat{u}}{\partial \tau}\right]\frac{\partial h^\circ}{\partial \tau} = (\hat{u}'''-\hat{u})\frac{\partial^2 h^\circ}{\partial \tau^2} - \hat{u}\frac{\hat{u}'''}{\hat{u}'}\frac{\hat{u}'}{\hat{u}''}\frac{dh_w}{dS_2}\operatorname{erfc}\left(\frac{\tau}{\sqrt{4S_3}}\right) \tag{36}$$

As in the element conservation equations, it is convenient to determine $\hat{u}'''$ in terms of $\hat{u}'$; therefore, it is unnecessary at this point to know C.

In Ref. 2 (cf p. 1 eq. 1), the condition for $\hat{u}'''$ or, in their notation, $d\xi_2' \equiv \hat{u}'''dS$ gives as an implicit restriction on the allowable values of $\hat{u}_j$, $\left(h^\circ_j / h^\circ_e\right)$, and $\left(h_{w(o)} / h^\circ_e\right)$, viz:

$$\delta^2 + (1-\beta^2)\cdot\delta - 2\alpha\beta\delta^{1/2} - \alpha^2 = 0$$

where α and β are functions of $\frac{h^\circ_j}{h^\circ_e}$, $\frac{h_{w(o)}}{h^\circ_e}$ and u_j, and $\delta = \left(\frac{d\xi_2}{d\xi'}\right)_o$ (i.e. at S, S_2, $S_3 = 0$).

V. HEAT TRANSFER

The local heat transfer at the wall, in the absence of mass diffusion at its surface, may be determined by:

$$q = -K_T \left(\frac{\partial T}{\partial Y}\right)_w = -\frac{\mu_e C}{\frac{\rho_j}{\rho_e} a} \left(\frac{\partial h^\circ}{\partial \tau}\right)_w \tag{37}$$

$$= -\frac{\mu_e C}{\frac{\rho_j}{\rho_e} a} (\pi S_3)^{-1/2} \left[(h^\circ_j - h_w(S_2)) + (h^\circ_e - h^\circ_j) \exp\left(-\frac{1}{4S_3}\right) \right]$$

$C = C(S_2)$ is determined from the species mass fraction solutions and from the wall temperature distribution

$$C = \frac{\rho_w \mu_w}{\rho_e \mu_e} \tag{38}$$

also

$$\frac{\rho_w}{\rho_j} = \frac{T_j}{T_w} \frac{W_w}{W_j}, \quad W = W_2, \qquad \frac{1}{W_w} = \sum_{i=1}^{4} \frac{Y_{i_w}}{W_i}$$

The viscosity μ_w may be found from the following viscosity formula for mixtures (see Ref. 5).

$$\mu_w = \sum_{i=1}^{4} \frac{\mu_{i_w} Y_{i_w}}{Y_{i_w} + W_i \sum_{\substack{j=1 \\ j \neq i}}^{4} \frac{Y_{j_w}}{W_j} \Phi_{ij}} \tag{39}$$

$$\Phi_{ij} = \frac{\left[1 + \left(\frac{\mu_{i_w}}{\mu_{j_w}}\right)^{1/2} \left(\frac{W_j}{W_i}\right)^{1/4}\right]^2}{\sqrt{2}\left[1 + \frac{W_i}{W_j}\right]^{1/2}}$$

Calculations are presented only for the constant wall temperature condition. For a nonuniform wall temperature distribution, φ_{i_j} must be found at every streamwise station. Additionally, the wall enthalpy distribution, h_w, will differ with the wall temperature distribution and hence the relation between S_3 and S is dependent upon this distribution; however, in the case of constant h_w, as already pointed out, $S_3 = S$.

A. Comparison With Flat Plate (No Slot):

The slot flow solution reduces to the flat plate with no injection when $\hat{u}_j = 1$, $h^\circ_j = h^\circ_e$; the composition being taken as that in the free stream.

For the constant wall temperature case, $h_w(o)$ is also the constant wall enthalpy of the flat plate problem. The total enthalpy solution for the case of the flat plate is given by the constant wall enthalpy solution, and by virtue of the Crocco relation, no separate collocation is necessary.

For the flat plate, the heat transfer is:

$$q' = - \frac{\rho_w' \mu_w'}{\rho_e a} \left(\frac{1}{2} S'\right)^{-1/2} \left(h^\circ_e - h'_w\right) \qquad (40)$$

where ' refers to quantities associated with the flat plate without slot injection.

Since the coordinate stretch is constant,

$$S' = \frac{1}{Re_a \hat{u}'} \frac{X}{a} \; ; \; Re_a = \frac{\rho_e u_e a}{\mu_e} \qquad (41)$$

and the heat transfer for the flat plate may be written as

$$- \frac{\left(\chi/\rho_e \mu_e u_e\right)^{1/2}}{h^o_e - h_{w'}} \qquad q' = \left(\frac{\hat{u}'}{\pi}\right)^{1/2} \tag{42}$$

which is also within 3% of the Blasius result for the flat plate.

The ratio of hydrogen injection heat transfer to flat plate heat transfer is therefore

$$\frac{q}{q'} = \frac{\rho_e \mu_e C}{\rho_j \mu_{w'}} \quad \frac{\rho_e}{\rho_{w'}} \left(\frac{S_3}{S'}\right)^{1/2} \left[\frac{h^o_j - h_w(S_2)}{h^o_e - h_{w'}} + \frac{h^o_e - h^o_j}{h^o_e - h_{w'}} \quad \exp\left(-\frac{1}{4S_3}\right)\right] \tag{43}$$

VI. CHOICE OF LINE OF COLLOCATION

In this paper a variant of the method of collocation is used to solve a non-similar problem. Schetz (cf Ref. 6) has applied the collocation technique to some similar and non-similar problems. Following Schetz(6) in the similarity case, the approximate solution to an equation is improved by determining a coordinate transformation which allows satisfaction of the equation at a particular value of the independent variable and determines a constant coordinate stretching factor; in particular (in Ref. 6), the point at which the solution is collocated is chosen to be a typical point of the range of the independent variable, (i.e. near the "middle" of the region). In the case of similar boundary layers, it is possible to choose a value of the similarity parameter $\frac{\tau}{\sqrt{4S}}$ such that the skin friction and heat transfer agree with the exact solution to the equations. Since the slot problem is inherently non-similar, it is not possible to choose a single value of $\frac{\tau}{\sqrt{4S}}$, but one must specify the value of S at the point of collocation; strict application of Shetz' procedure would imply this choice. However, it is possible to choose a $\frac{\tau}{\sqrt{4S}}$ value for each value of S, thereby determining a variable coordinate stretch factor. That a rational basis for choosing $\frac{\tau}{\sqrt{4S}}$ as a function of S exists, may be seen from the following argument: the wall boundary layer, which is assumed initially zero, must behave, for small S as a similar boundary layer whose external flow is that of the jet issuing from the slot. Far downstream, the layer must behave as a similar boundary layer with the freestream flow for external conditions. In both instances, the

results of Schetz for similar boundary layers indicate collocation should be applied at the same value of $\frac{\tau}{\sqrt{4S}} = t$.

In some respects, the layer adjacent to the wall may be viewed as a boundary layer with varying outer conditions; then to recover the solution for small and large S, the method of choosing must recover the value of t appropriate to the similar boundary layer (Blasius). Also, as $\hat{u}_j \to 1$, $h_j^\circ \to h_e^\circ$ and $\tilde{Y}_{i_j} \to \tilde{Y}_{i_e}$, the Blasius result must be recovered.

Choosing t as a constant function of S equal to the Blasius value of t is not sufficient since, at a given t, the profile characteristics change with S; in particular, the ratio of $\left\{\frac{\partial^2 \hat{u}}{\partial \tau^2} \Big/ \frac{\partial \hat{u}}{\partial \tau}\right\}$ changes sign by passing through zero. The coordinate stretch condition shows this to be a singlular point. Thus unappealing result may be avoided by collocating at a value of t (S) at which the layer has similar characteristics. Since most of the layer has negative values of $\left\{\frac{\partial^2 \hat{u}}{\partial \tau^2} \Big/ \frac{\partial \hat{u}}{\partial \tau}\right\}$ collocation is applied at values of t for which the ratio has a negative sign.

In the similar boundary layer $\sqrt{S}\left\{\frac{\partial^2 \hat{u}}{\partial \tau^2} \Big/ \frac{\partial \hat{u}}{\partial \tau}\right\}$ has a constant value for any given value of t. Thus, choosing t so that $\sqrt{S}\left\{\frac{\partial^2 \hat{u}}{\partial \tau^2} \Big/ \frac{\partial \hat{u}}{\partial \tau}\right\}$ has the value found in the collocation of the Blasius case, will assure the desired behavior of t (S). This is equivalent to collocating along a line in the flow at which the profiles have an important characteristic kept constant.

The total enthalpy solution is also treated in the manner described above; in general, the momentum and energy equations are not collocated along the same lines.

The element mass fraction solutions show a different character; the ratio $\left| \frac{\partial^2 \tilde{Y}_i}{\partial \tau^2} \Big/ \frac{\partial \tilde{Y}_i}{\partial \tau} \right|$ does not have a behavior similar to that of the velocity and total enthalpy solutions, but has a positive sign near the wall and a negative sign far from the wall. The sign changes always occur above a minimum value of $t_2 = \sqrt{2}/2$. Since the solutions are collocated to obtain the correct wall behavior, the element mass fraction solution is collocated at a specific value of $t_2(S) < t_2$ in the region near the wall. Comparison with the results of Ref. 2 indicate $t_2 \cong .35$ along the line of collocation for the specie continuity equation.

VII. COORDINATE STRETCH FACTORS

In the local collocation procedure, the coordinate stretch factors u, u'' and u''' are functions of S; hence, the conditions for the factors may be looked upon as differential equations for the S_2 and S_3 coordinates as functions of S. With some rearranging, the conditions may be written as:

Chemistry Condition

$$\frac{dS_2}{dS} = \frac{1}{\hat{u}} \left[\hat{u}'(S) - \left\{ \left(\frac{\partial \hat{u}}{\partial \tau} \right)_w - \frac{\partial \hat{u}}{\partial \tau} \right\}_{t = t'_2 \sqrt{\frac{S_2}{S}}} \left(\frac{\partial \tilde{Y}_i}{\partial \tau} \Big/ \frac{\partial^2 \tilde{Y}_i}{\partial \tau^2} \right)_{t_2 = t'_2} \right]$$

$$\hat{u} = \hat{u}\left(S, t'_2 \sqrt{\frac{S_2}{S}}\right) \qquad (44)$$

at S, $S_2 = 0$

$$\frac{dS_2}{dS} = \hat{u}' \Big/ \hat{u}_j \ \text{erf}\left(t'_2 \sqrt{\frac{dS_2}{dS}}\right)$$

Enthalpy Condition

$$\frac{dS_3}{dS} = \frac{1}{\hat{u}} \left[\hat{u}'(S) - \left\{ \left(\frac{\partial \hat{u}}{\partial \tau} \right)_w \frac{\partial \hat{u}}{\partial \tau} \right\}_{t = t_3' \sqrt{\frac{S_3}{S}}} \frac{\partial h^\circ}{\partial \tau} \Big/ \frac{\partial h^\circ}{\partial \tau^2} \right.$$

$$\left. - \hat{u} \frac{dS_2}{dS} \frac{dh_w}{dS_2} \ \text{erfc}(t'_3) \Big/ \frac{\partial^2 h^\circ}{\partial \tau^2} \right]_{t'_3}$$

$$\hat{u} = \hat{u}\left(t'_3 \sqrt{\frac{S_3}{S}}\right)$$

at S, S_2, $S_3 = 0$

$$\frac{dS_3}{dS} = 1$$

Evaluated at t_3 such that $\left(\frac{\partial h^\circ}{\partial \tau} \Big/ \frac{\partial^2 h^\circ}{\partial \tau^2} \right)^{-1/2} = \text{constant} = 1/.7$

$\hat{u}'(S)$ is determined from the velocity condition

$$\hat{u}' = \hat{u} + \left\{ \left(\frac{\partial \hat{u}}{\partial \tau} \right)_w - \frac{\partial \hat{u}}{\partial \tau} \right\} \left(\frac{\partial \hat{u}}{\partial \tau} \Big/ \frac{\partial^2 \hat{u}}{\partial \tau^2} \right) \tag{46}$$

evaluated at t such that $\left(\frac{\partial \hat{u}}{\partial \tau} \Big/ \frac{\partial^2 \hat{u}}{\partial \tau^2} \right)_s^{-1/2}$ = constant = 1/.7.

Solutions to the equations were obtained by numerical integration on a Bendix G15 computer by the Kutta-Runge-Gill method with variable step-size selected by a curvature criterion. A range of parameters was selected and the results for one choice are compared with computations obtained by the method of Libby and Schetz (cf Ref. 2).

DISCUSSION OF RESULTS

Calculations were carried out at a particular point along a typical Launch Trajectory. Previous estimates (i.e., Ref. 1) indicate that the minimum delay lengths associated with the Hydrogen occur at altitudes of about 45 kilometers; therefore, most of the calculations were performed at an altitude of 45k.m., at an ambient temperature of 275.8° k, and ambient pressure of 0.00157 atmosphere. The vehicle velocity was 5780 ft/sec. Heat transfer results are shown in Figures 2A - 2K.

The idealizations employed in this report have some consequences on the applicability of the analysis. Thus, the simplifications of laminar, constant pressure flow restrict this study to high altitude conditions or other regimes where it is resonable to expect laminar flow. The choice of unity Prandtl and Lewis numbers are justified by the simplicity of the subsequent analysis. The assumption of equilibrium chemistry and the flame sheet model there to requires that static temperature and pressure levels be sufficiently elevated to insure a reaction time small in comparison with characteristic flow times; however, since localized conditions on the missile can generate shocks and hot boundary layers along the vehicle surface, reations may be initiated and be sustained by the subsequent heat release. Most of the calculations performed herein contained initial static conditions which indicate reation times comparable to characteristic flow times; hence, the corresponding equilibrium chemistry calculations must be regarded as being initiated by a local higher temperature region near the lip of the slot. A calculation shown in Figure 2J was performed for a higher external temperature so that the self-ignition and equilibrium chemistry conditions were attained.

In general, results of the analysis indicate that choice of the velocity ratio $\hat{u}_j$ is relatively unimportant in determining the overall length of the reation zone (flame length). This is in contradistinction with the results obtained for free jets as reported in Ref. (7). The lack of sensitivity is due to the relatively short region of influence of the jet flow on the wall layer compared to that of the external flow, i.e., the boundary layer due to the jet is quictly submerged. The flame length, x^*, is the directly proportional to $aRe_a\left(\rho_j/\rho_e\right)^2$, that is, holding the external conditions constant, x^* is proportional to the square of the slot height and jet density ratio. The region of heat transfer reduction scales in a similar way.

Results for various jet velocity ratios indicate that, for equilibrium chemistry flames, reduction of that ratio reduces heat transfer uniformly over the region close to the slot, i.e., where the heat transfer ratio is less than unity, until some small velocity ratio; further reductions in the velocity ratio result in a heat transfer increase at some distance from the slot. The principal cause for this may be seen in the variation of the extent of the region of heat transfer reduction; for jet velocity ratios decreasing from unity the region grows until a velocity ratio of $1/3 \approx 1/2$ is reached and thereafter decreases with further reduction in velocity ratio. This behavior, in turn, is due to the increased heat transfer into the jet flow from the external stream as the jet velocity ratio, $\hat{u}_j = u_j / u_e$ decreases, eventually increasing the jet flow temperature and hence, the heat transfer to the body.

The length variation of the reduced heat transfer region and the variation of peak heat transfer ratio with velocity ratio were of the order of 20% while the flame length was relatively unaffected by the jet velocity ratio. This occured because the velocity and element mass reaction solutions settled down to that

corresponding to the $u_j/u_e = 1$ case in distances much shorter than the flame length; however, the enthalpy solution required much longer distances due to the variations in the wall enthalpy and flow field temperatures caused by the chemical reactions.

The frozen chemistry calculations corresponding to the same initial conditions and wall temperature as the equilibrium chemistry computations are shown on the same figures. In general, the heat transfer ratio goes smoothly from its value at the slot to the downstream asymptotic value in distances comparable to the flame length of the corresponding equilibrium case.

The heat transfer ratio distribution for the jet velocity ratio of 2 shown in Figure 2K exhibits the effects of an energy transfer from the jet flow to the external flow field. In this case, it is noted that the relative values of the conductivities of hydrogen and air offset the increase in total external enthalpy seen by the wall layer so that initially, the heat transfer ratio was approximately unity. Even so, the appearance of the large heat transfer rate associated with combustion was delayed considerably. And, in the event of no occurence of combustion a reduction in the heat transfer was found.

Figures 2F-H, illustrate the large effect of the jet density ratio $\left(\frac{\rho_j}{\rho_e}\right)$ on the flame length. Figure 2I shows the smaller effect of the wall temperature.

In Figure 3 a comparison is shown between the present results and those of Libby and Scheetz (i.e., Ref. 2) for equilibrium chemistry. There is a substantial agreement between the two analyses.

Some typical properties of the constant wall temperature solution are shown in Figures 4-8.

In sum, the results illustrate the advantages of injecting cold gases into the boundary layers of launch vehicles. In many cases, reactions may be assumed to occur, and it is seen that the heat transfer rise associated with combustion occuring close to the body may be delayed for substantial distances downstream from a slot injector and occurs in a region of relatively low heat transfer. For a given mass flow of material and a given slot height , it seems desirable to inject a cold, and, hence, dense gas. (It is noted that this implies a correspondingly low injection velocity.)

REFERENCES

1. Libby, P. A., Pergament, H. S., Taub, P. A., Engineering Estimates of Flow Lengths Associated with Launch Trajectory, GASL Technical Report TR-330, December 1962.

2. Libby, P. A., Schetz, J. A., Approximate Analysis of Slot Injection of a Reactive Gas in Laminar Flow, GASL Technical Report TR-293, November 1962 .

3. Cohen, C. E., Bromberg, R., and Lipkis, R. P., Boundary Layer With Chemical Reaction Due to Mass Addition, Jet Propulsion, Vol. 28, No. 10, pp. 659-668, October 1958.

4. Carslaw, H. S., and Jaeger, J. C., Conduction of Heat in Solids, Oxford University Press, Second Edition 1953.

5. Bromley, L. A., and Wilke, C. R., Viscosity Behavior of Gases, Industrial and Engineering Chemistry, Vol. 43, Page 1641, July 1951.

6. Schetz, J. A., On the Approximate Solution of Viscous Flow Problems. (To be presented at the Summer Conference of Applied Mechanics Division, Ithaca, New York, June 24-26, 1963. ASME Paper No. 63 - APM-3.)

7. Libby, P.A., and Rosenbaum, H., Axisymmetric Laminar And Turbulent Jets of Hydrogen With Simple Chemistry, GASL TR-331

APPENDIX I

Exact Rayleigh-Stokes Problem:

It has been seen that by a local similarity assumption, the solution to the Rayleigh-Stokes problem associated with the constant wall enthalpy case can be adapted to a nonuniform wall enthalpy problem (the constant wall temperature case, for example). The solution to the Rayleigh-Stokes problem associated with an arbitrary wall enthalpy distribution may be derived. It will be shown that the heat transfer at the wall is close to that given by the local similarity solution.

Considering the variable $H = h^\circ - h_{w_o}$, the equations and boundary conditions for the related Rayleigh problem is:

$$\frac{\partial H}{\partial S_4} - \frac{\partial^2 H}{\partial \tau^2} = 0$$

Satisfying:

$$\begin{aligned} &\tau = 0: && H = H_w = h_w - h_{w_o} \\ &\tau \to \infty: && H = H_e = h^\circ_e - h_{w_o} \\ &S_4 = 0: && 0 < \tau \le 1 \; ; \; H = H_j = h^\circ_j - h_{w_o} \\ & && \tau > 1 \; ; \; H = H_e \end{aligned} \qquad (1)$$

This is broken into two problems which, when superimposed, satisfy all the boundary conditions.

1. H_o satisfies the equations and the following boundary conditions:

$$\begin{aligned} &\tau = 0 && H_o = 0 && S_4 = 0: \; 0 < \tau \le 1; \; H_o = H_j \\ &\tau \to \infty && H_o = H_e && \tau > 1 \; ; \; H_o = H_e \end{aligned} \qquad (2)$$

2. H_1 satisfies the equation and the conditions:

$$\begin{aligned} \tau = 0: &\qquad H_1 = H_w \\ \tau \to \infty: &\qquad H_1 = 0 \\ S_4 = 0: &\qquad H_1 = 0 \end{aligned} \tag{3}$$

The solution for H_1 is obtained by Duhamel's principle from the solution to Problem 2 where

$$H_1 \ (\tau = 0) = 1$$

Hence the solution to the exact related Rayleigh-Stokes problem is:

$$h^\circ = h_{w_o} + \left(h_j^\circ - h_{w_o}\right) \operatorname{erf}\left(\frac{\tau}{\sqrt{4S_4}}\right) + \frac{h_e^\circ - h_j^\circ}{2}\left[\operatorname{erf}\left(\frac{\tau-1}{\sqrt{4S_4}}\right) + \operatorname{erf}\left(\frac{\tau+1}{\sqrt{4S_4}}\right)\right]$$
$$+ \frac{4}{\tau\sqrt{\pi}} \int_0^{S_4} \left(h_w(\lambda) - h_{w_o}(S_4)\right) \left(\frac{\tau}{\sqrt{4(S_4-\lambda)}}\right)^3 \exp\left(\frac{-\tau^2}{4(S_4-\lambda)}\right) d\lambda \tag{4}$$

and since

$$\frac{4}{\tau^2\sqrt{\pi}} \int_0^{S_4} \left(\frac{\tau}{\sqrt{4(S_4-\lambda)}}\right)^3 \exp\left(-\frac{\tau^2}{4(S_4-\lambda)}\right) d\lambda = \operatorname{erfc}\left(\frac{\tau}{\sqrt{4S_4}}\right)$$

This solution may be written as

$$h^\circ = h_w + (h_j^\circ - h_w) \operatorname{erf}\left(\frac{\tau}{\sqrt{4S_4}}\right) + \frac{h_e^\circ - h_j^\circ}{2}\left[\operatorname{erf}\left(\frac{\tau-1}{\sqrt{4S_4}}\right) + \operatorname{erf}\left(\frac{\tau+1}{\sqrt{4S_4}}\right)\right]$$
$$+ \frac{4}{\tau^2\sqrt{\pi}} \int_0^{S_4} \left(h_w(\lambda) - h_w(S_4)\right) \left(\frac{\tau}{\sqrt{4(S_4-\lambda)}}\right)^3 \exp\left(-\frac{\tau^2}{4(S_4-\lambda)}\right) d\lambda \tag{5}$$

or

$$h^\circ = h^\circ_{L.S.} + \frac{4}{\tau^2\sqrt{\pi}} \int_0^{S_4} \left(h_w(\lambda) - h_w(S_4)\right) \left(\frac{\tau}{\sqrt{4(S_4-\lambda)}}\right)^3 \exp\left(-\frac{\tau^2}{4(S_4-\lambda)}\right) d\lambda$$

(6)

where $h^{o}_{L.S}$ is the local similarity result.

The general distribution of wall enthalpy may be locally approximated by the Taylor series valid in the segment $S_{i-1} \leq S \leq S_i$. The contribution of any particular segment to the integral term in Eq. 6 may be evaluated as follows:

Define

$$I_i = \frac{4}{\tau^2\sqrt{\pi}} \int_{S_{4_{i-1}}}^{S_{4_i}} h_w(\lambda) \left(\frac{\tau}{\sqrt{4(S_4-\lambda)}}\right)^3 \exp\left(\frac{-\tau^2}{\sqrt{4(S_4-\lambda)}}\right) d\lambda$$

By expanding $h_w(\lambda)$, the integral can be approximated as

$$I_i \cong \left[A_{i-1} + \frac{B_{i-1}\tau^2}{2} + \frac{h''_{w_{i-1}}\tau^4}{24}\right] \operatorname{erfc}\left(\frac{\tau}{\sqrt{4(S_4-S_{4_{i-1}})}}\right) - \operatorname{erfc}\left(\frac{\tau}{\sqrt{4(S_4-S_{4_i})}}\right)$$

$$- \frac{1}{\sqrt{\pi}}\left[\frac{B_{i-1}\tau^2}{2} + \frac{h''_{w_{i-1}}\tau^4}{24}\right]\left[\frac{\sqrt{4(S_4-S_{4_{i-1}})}}{\tau} \exp\left(\frac{-\tau^2}{4(S_4-S_{4_{i-1}})}\right) - \frac{\sqrt{4(S_4-S_{4_i})}}{\tau} \exp\left(\frac{-\tau^2}{4(S_4-S_{4_i})}\right)\right]$$

$$+ \frac{h''_{w_{i-1}}\tau^4}{48\sqrt{\pi}}\left[\left(\frac{4(S_4-S_{4_{i-1}})}{\tau^2}\right)^{3/2} \exp\left(\frac{-\tau^2}{4(S_4-S_{4_{i-1}})}\right) - \left(\frac{4(S_4-S_{4_i})}{\tau^2}\right)^{3/2} \exp\left(\frac{-\tau^2}{4(S_4-S_{4_i})}\right)\right]$$

where $$A = h_{w_{i-1}} + (S_4-S_{4_{i-1}})\, h'_{w_{i-1}} + \frac{1}{2}(S_4-S_{4_{i-1}})^2\, h''_{w_{i-1}}$$

$$B = h'_{w_{i-1}} + (S_4-S_{4_{i-1}})\, h''_{w_{i-1}}$$

$$h_{w_{i-1}} \equiv h_w(S_{4_{i-1}})$$

$'$ Denotes $\frac{d}{dS_4} = \frac{dS_2}{dS_4}\frac{d}{dS_2}$

and $h_w(\lambda)$ has been expanded as:

$$h_w(\lambda) \cong h_{w_{i-1}} + (\lambda - S_{4_{i-1}})\, h'_{w_{i-1}} + \frac{1}{2}(\lambda - S_{4_{i-1}})^2\, h''_{w_{i-1}}$$

and it was noted that

$$\lambda - S_{4_{i-1}} = (\lambda - S_4) + (S_4 - S_{4_{i-1}})$$

The integral

$$I = \frac{4}{\tau^2 \sqrt{\pi}} \int_0^{S_4} h_w(\lambda) \left(\frac{\tau}{\sqrt{4(S_4 - \lambda)}} \right)^3 \exp\left(\frac{-\tau^2}{\sqrt{4(S_4 - \lambda)}} \right) d\lambda$$

may, therefore, be approximated by summing the contributions from all preceeding segments

eg:

$$I = \sum_{i=1}^{n} I_i$$

where $S_{4_n} \equiv S_4$

The integral term in Eq. 6 is simply

$$I = h_w \operatorname{erfc}\left(\frac{\tau}{\sqrt{4 S_4}} \right)$$

The heat transfer, being proportional to $\left(\frac{\partial h^o}{\partial \tau} \right)$, may be examined by consideration of that quantity.

$$\left(\frac{\partial h^o}{\partial \tau}\right) = \left(\frac{\partial h^o}{\partial \tau}\right)_{L.S.} + \frac{1}{\sqrt{\pi}} \int_o^{S_4} \frac{\left(h_w(\lambda) - h_w(S)\right)}{2(S_4-\lambda)^{3/2}} \left[1 - \frac{1}{2} \frac{\tau^2}{(S_4-\lambda)}\right] \exp\left(\frac{-\tau^2}{4(S_4-\lambda)}\right) d\lambda$$

or, by using the approximation to the integral of equation 6:

$$\left(\frac{\partial h^o}{\partial \tau}\right) = \left(\frac{\partial h^o}{\partial \tau}\right)_{L.S.} + \frac{\partial}{\partial \tau}\left(I - h_w \operatorname{erfc}\left(\frac{\tau}{\sqrt{4S_4}}\right)\right)$$

$$= \left(\frac{\partial h^o}{\partial \tau}\right)_{L.S.} + \frac{h_w}{\sqrt{\pi S_4}} \exp\left(\frac{-\tau^2}{4S_4}\right) + \sum_{i=1}^{N} \frac{\partial I_i}{\partial \tau}$$

where, for $i \neq N$

$$\frac{\partial I_i}{\partial \tau} \cong \left[A_{i-1} + B_{i-1}\tau + h''w_{i-1}\frac{\tau^3}{6}\right]\left[\operatorname{erfc}\left(\frac{\tau}{\sqrt{4(S_4-S_{4_{i-1}})}}\right) - \operatorname{erfc}\left(\frac{\tau}{\sqrt{4(S_4-S_{4_{i-1}})}}\right)\right]$$

$$- \frac{2A_{i-1}}{\sqrt{\pi}}\left[\frac{1}{\sqrt{4(S_4-S_{4_{i-1}})}} \exp\left(\frac{-\tau^2}{4(S_4-S_{4_{i-1}})}\right) - \frac{1}{\sqrt{4(S_4-S_{4_i})}} \exp\left(\frac{-\tau^2}{4(S_4-S_{4_i})}\right)\right]$$

$$- \frac{1}{\sqrt{\pi}}\left[\frac{B_{i-1}}{2} + h''w_{i-1}\frac{\tau^2}{6}\right]\left[\sqrt{4(S_4-S_{4_{i-1}})} \exp\frac{-\tau^2}{4(S_4-S_{4_{i-1}})} - \sqrt{4(S_4-S_{4_i})} \exp\left(\frac{-\tau^2}{4(S_4-S_{4_i})}\right)\right]$$

$$+ \frac{h''w_{i-1}}{48\sqrt{\pi}}\left[\left(4(S_4-S_{4_{i-1}})\right)^{3/2} \exp\left(\frac{-\tau^2}{\sqrt{4(S_4-S_{4_{i-1}})}}\right) - \left(4(S_4-S_{4_i})\right)^{3/2} \exp\left(\frac{-\tau^2}{\sqrt{4(S_4-S_{4_i})}}\right)\right]$$

while for $i = N$

$$\frac{\partial I_N}{\partial \tau} \cong \left[A_{i-1} + B_{i-1}\tau + h''w_{i-1}\frac{\tau^3}{6}\right] \operatorname{erfc}\left(\frac{\tau}{\sqrt{4(S_4-S_{4_{N-1}})}}\right) - \frac{2A_{i-1}}{\sqrt{\pi}} \frac{\exp\left(\frac{-\tau^2}{4(S_4-S_{4_{N-1}})}\right)}{\sqrt{4(S_4-S_{4_{N-1}})}}$$

$$- \frac{1}{\sqrt{\pi}} \left[\frac{B_{i-1}}{2} + h''_{w_{i-1}} \frac{\tau^2}{6} \right] \sqrt{4\left(S_4 - S_{4_{N-1}}\right)} \exp\left(\frac{-\tau^2}{4\left(S_4 - S_{4_{N-1}}\right)} \right)$$

$$+ \frac{h''_{w_{i-1}}}{48\sqrt{\pi}} \left(4\left(S_4 - S_{4_{N-1}}\right)\right)^{3/2} \exp\left(\frac{-\tau^2}{4\left(S_4 - S_{4_{N-1}}\right)} \right)$$

For small τ, it is obvious that for slowly changing wall enthalpies, the heat transfer is close to the local similarity value. With this restriction, the two Rayleigh-Stokes problems approach each other (the coordinate stretching factors also tend to each other).

If the exact Rayleigh-Stokes solution were collocated, the collocation condition for determining S_4 would be:

$$\frac{dS_4}{dS} = \frac{1}{\hat{u}} \left[\hat{u}'(s) - \left(\frac{\partial \hat{u}}{\partial \tau}_w - \frac{\partial \hat{u}}{\partial \tau}_{t=t_4\sqrt{\frac{S_4}{S}}} \right) \left(\frac{\partial h^\circ}{\partial \tau} \middle/ \frac{\partial^2 h^\circ}{\partial \tau^2} \right) \right]$$

where $$\hat{u} = \hat{u}\left(t_4 \sqrt{\frac{S_4}{S}}\right)$$

and at $S, S_2, S_4 = 0$

$$\frac{dS_4}{dS} = 1$$

NOTATION

English

a	slot height in physical coordinates
C	non-dimensional $\rho\mu$ Prandtl $= \frac{\rho\mu}{\rho_e \mu_e}$
C_f	skin friction coefficient $= \tau_w / \rho_e u_e^2$
h	enthalpy
h^o	total enthalpy
$k = 0, 1$	indicates two dimensional or axisymmetric flow respectively
k_r	Thermal conductivity
q	heat transfer rate
r	body radius in axisymmetric coordinate system
R_{e_a}	Reynolds number - $\frac{\rho_e u_e a}{\mu_e}$
S_1, S_2, S_3	transformed streamwise coordinates
t	transformed Blasius variable $= \frac{\tau}{\sqrt{4S}}$
T	temperature
u	streamwise velocity
v	normal velocity
$\hat{u} = u/u_e$	streamwise velocity non-dimensionalized with respect to free stream conditions
v^*	transformed normal velocity
$\hat{v} = v^*/u_e$	transformed normal velocity non-dimensionalized with respect to free stream velocity
$\hat{u}', \hat{u}'', \hat{u}'''$	non-dimensional effective convective velocity
W	molecular weight
y	normal coordinate
Y	specie mass fraction
$\tilde{Y}$	element mass fraction

Greek

η_a	transformed slot height
μ	viscosity
ξ, ξ_2, ξ_3	transformed streamwise coordinates
τ	transformed normal coordinate
ρ	density

Subscripts

e	free stream conditions
f	conditions at flame sheet
F	conditions with frozen chemistry
j	conditions at slot
1	oxygen
2	hydrogen
3	water
4	nitrogen

Superscripts

*	denotes conditions where $\tau_f = 0$ (flame sheet impinges upon wall)

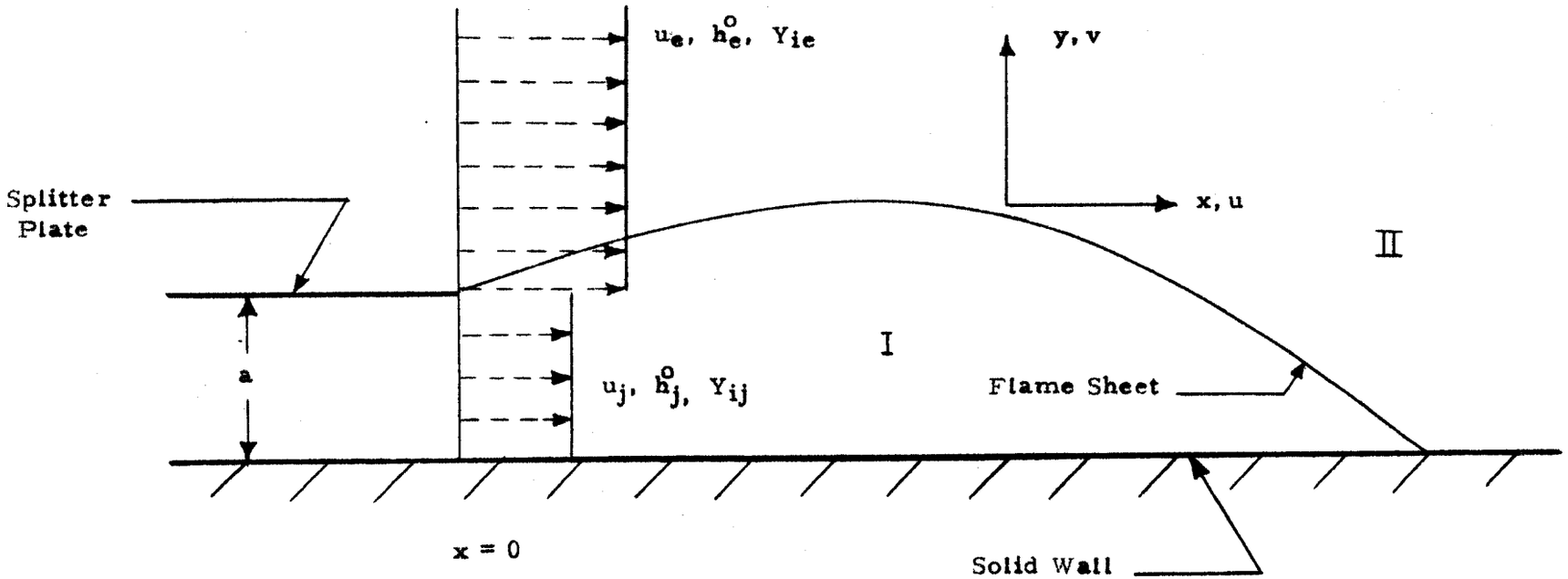

Figure 1 Schematic Representation of Flow Field

GASL
WESTBURY, N.Y.

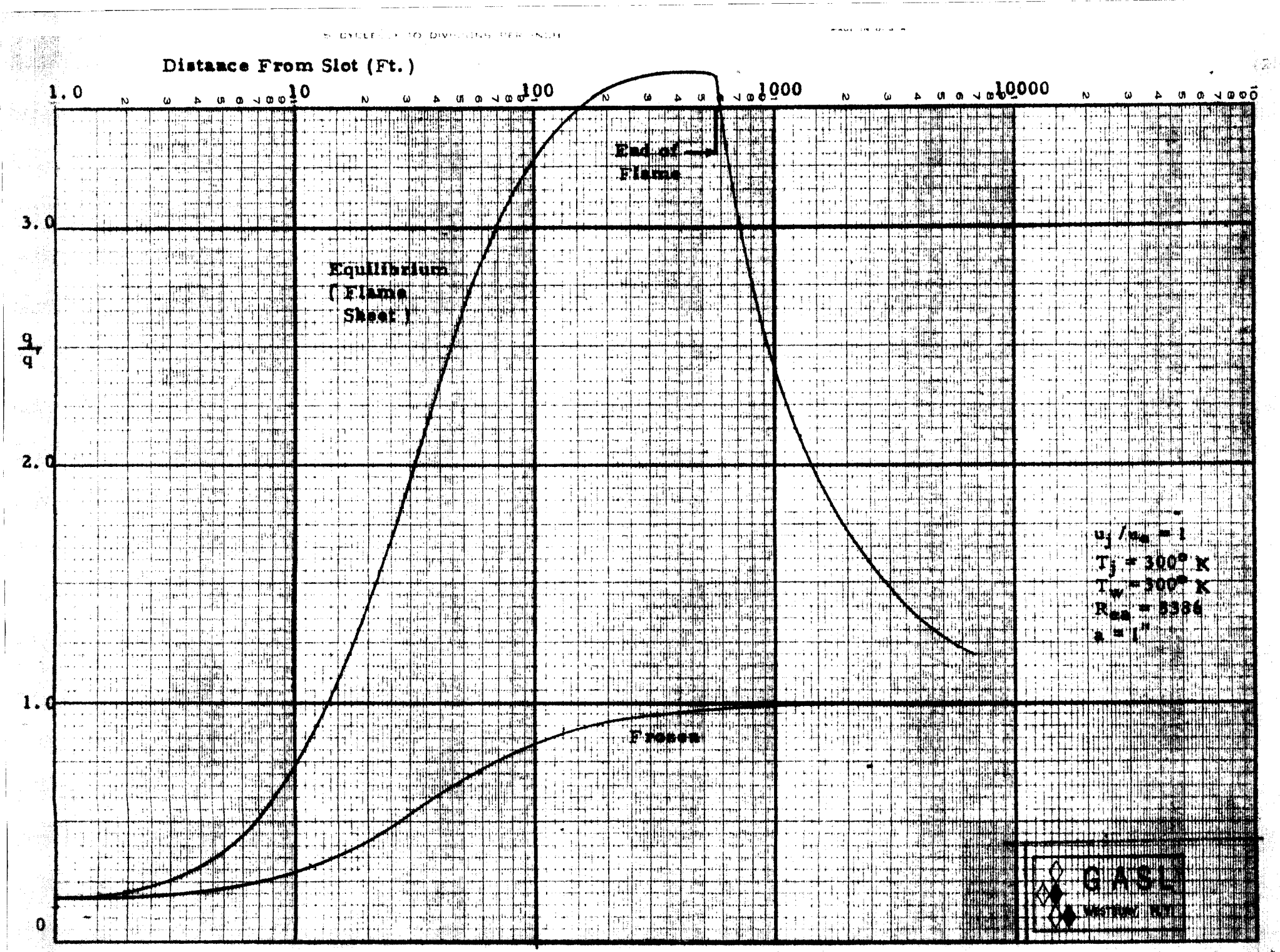

Figure 2A Heat Transfer Ratio

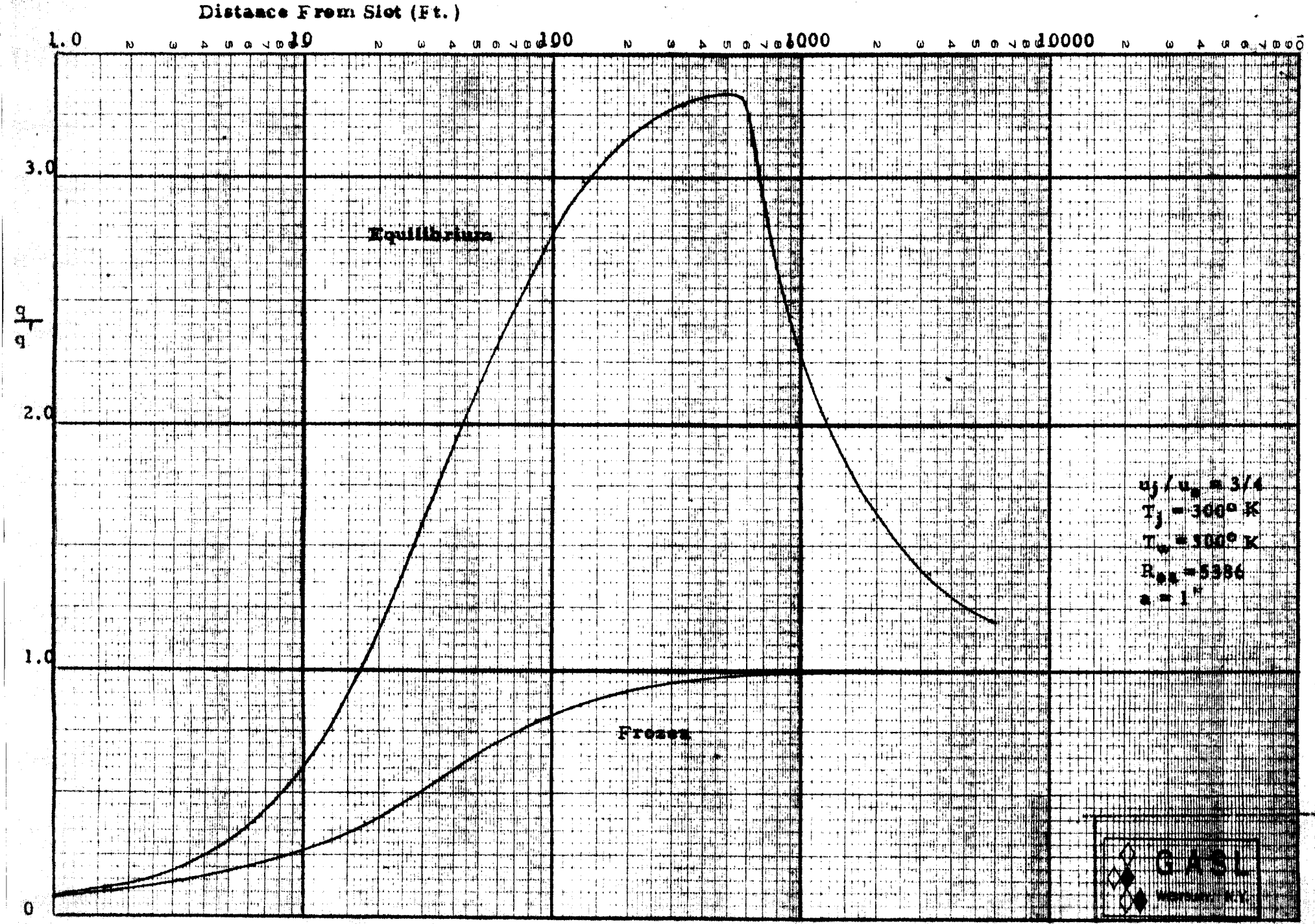

Figure 2B Heat Transfer Ratio

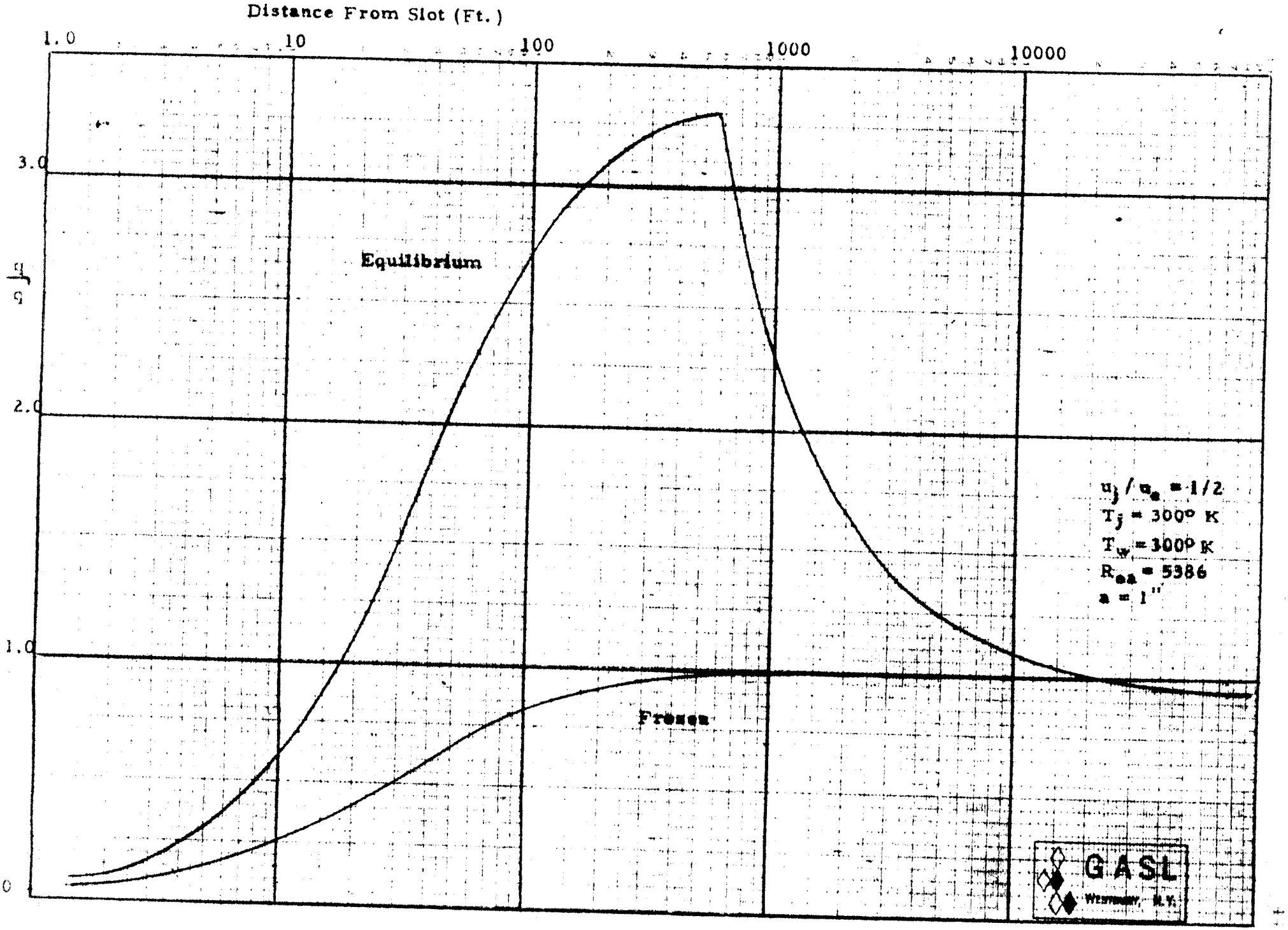

Figure 2C Heat Transfer Ratio

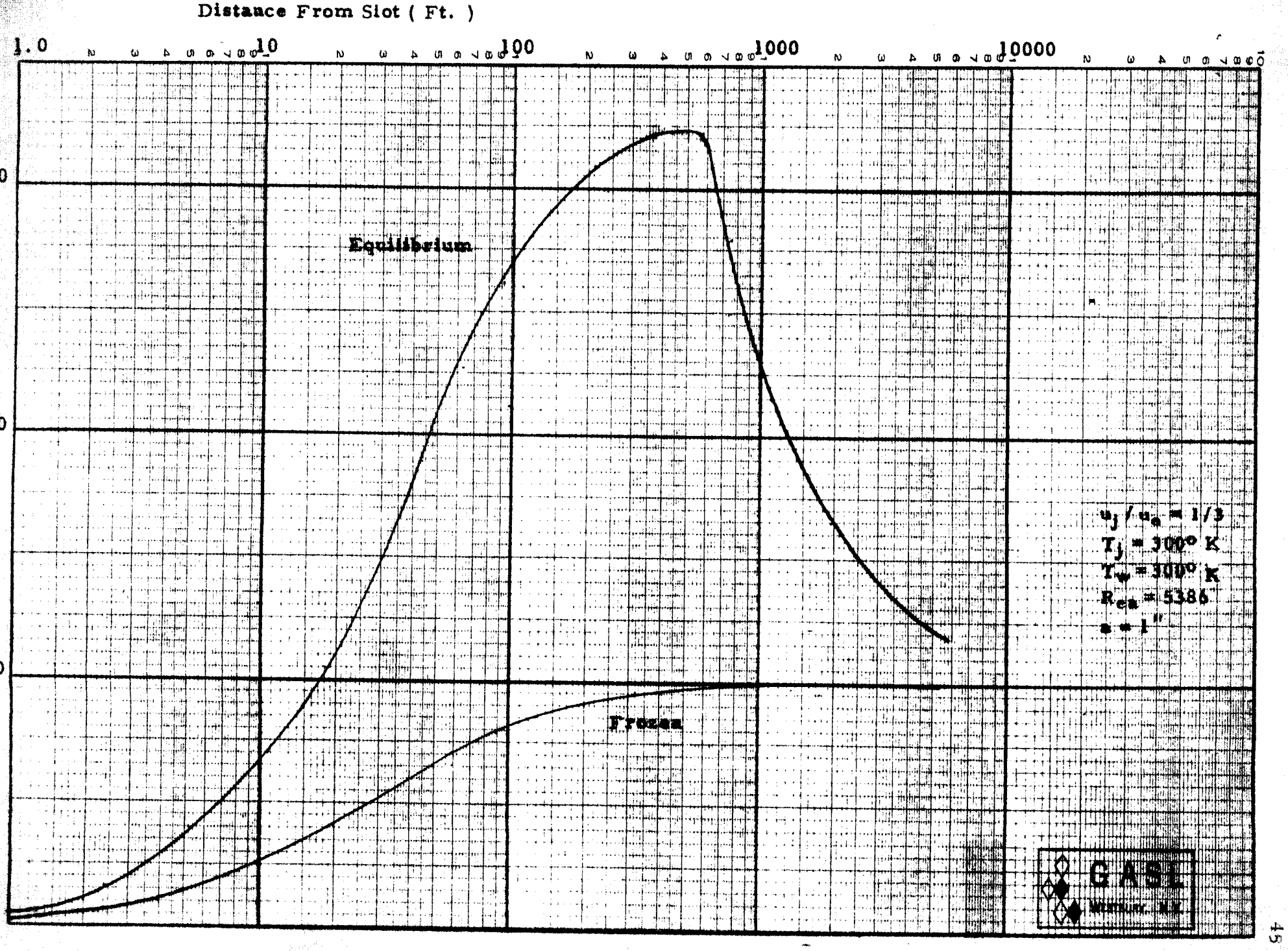

Figure 2D Heat Transfer Ratio

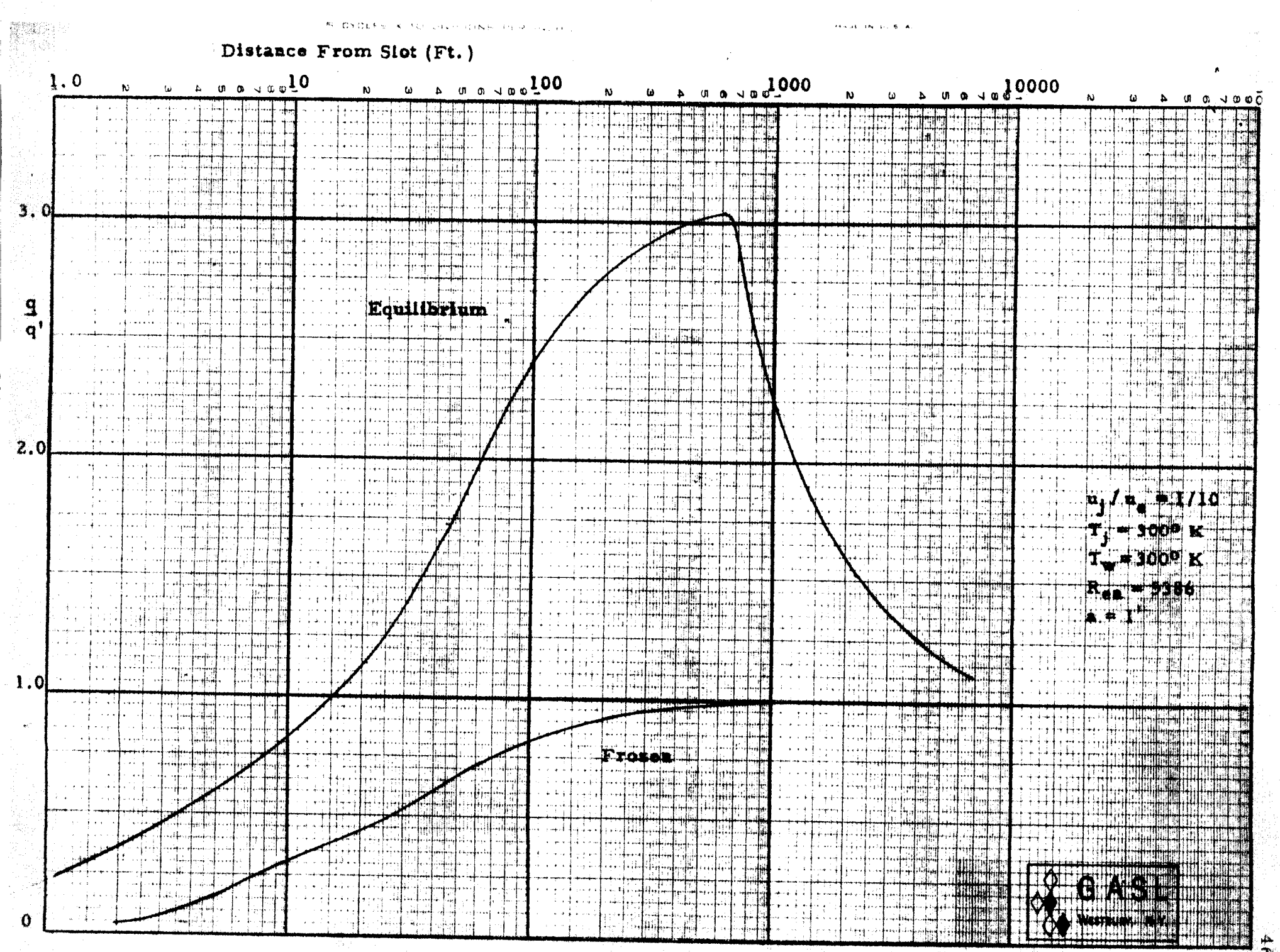

Figure 2E Heat Transfer Ratio

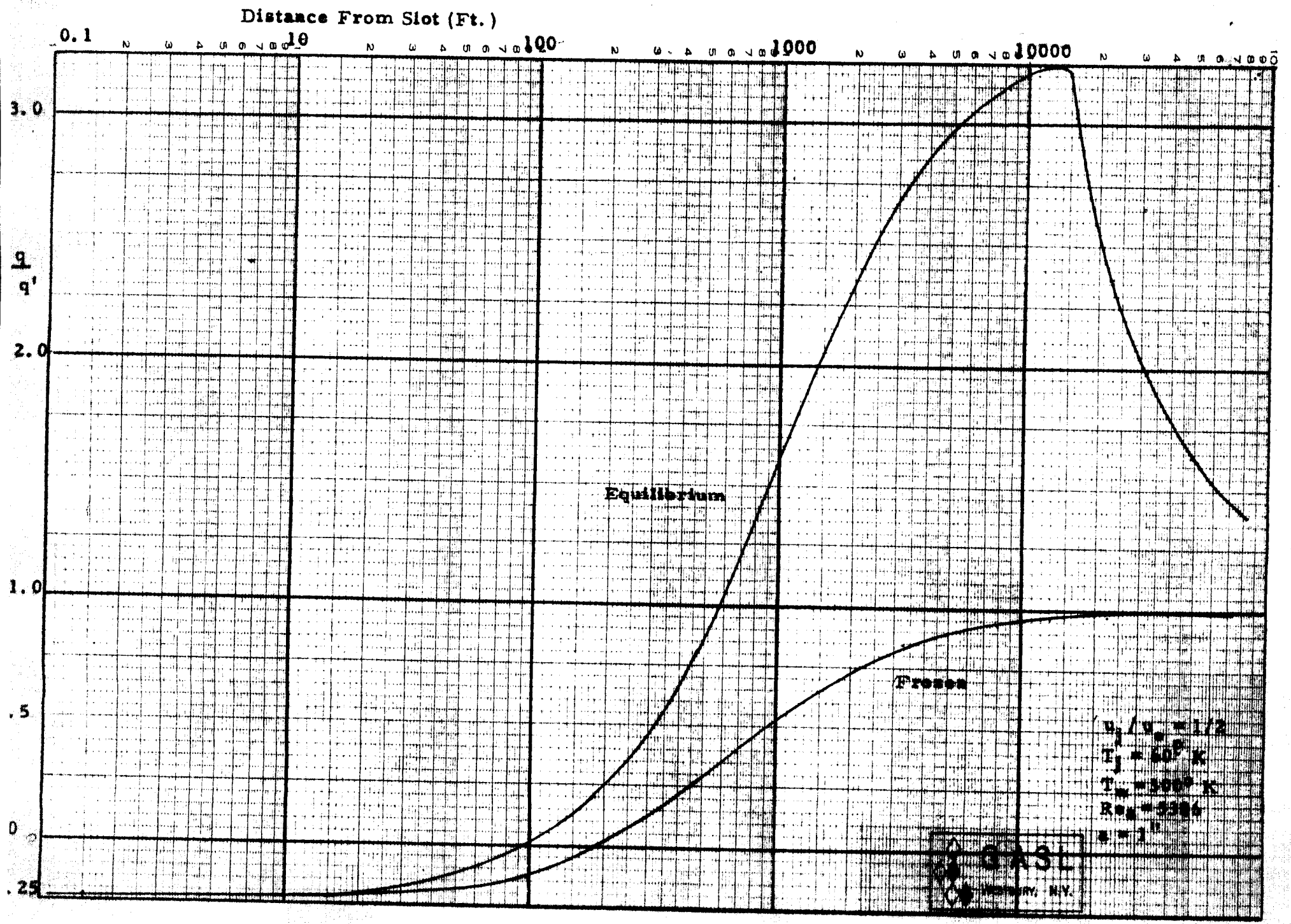

Figure 2F Heat Transfer Ratio

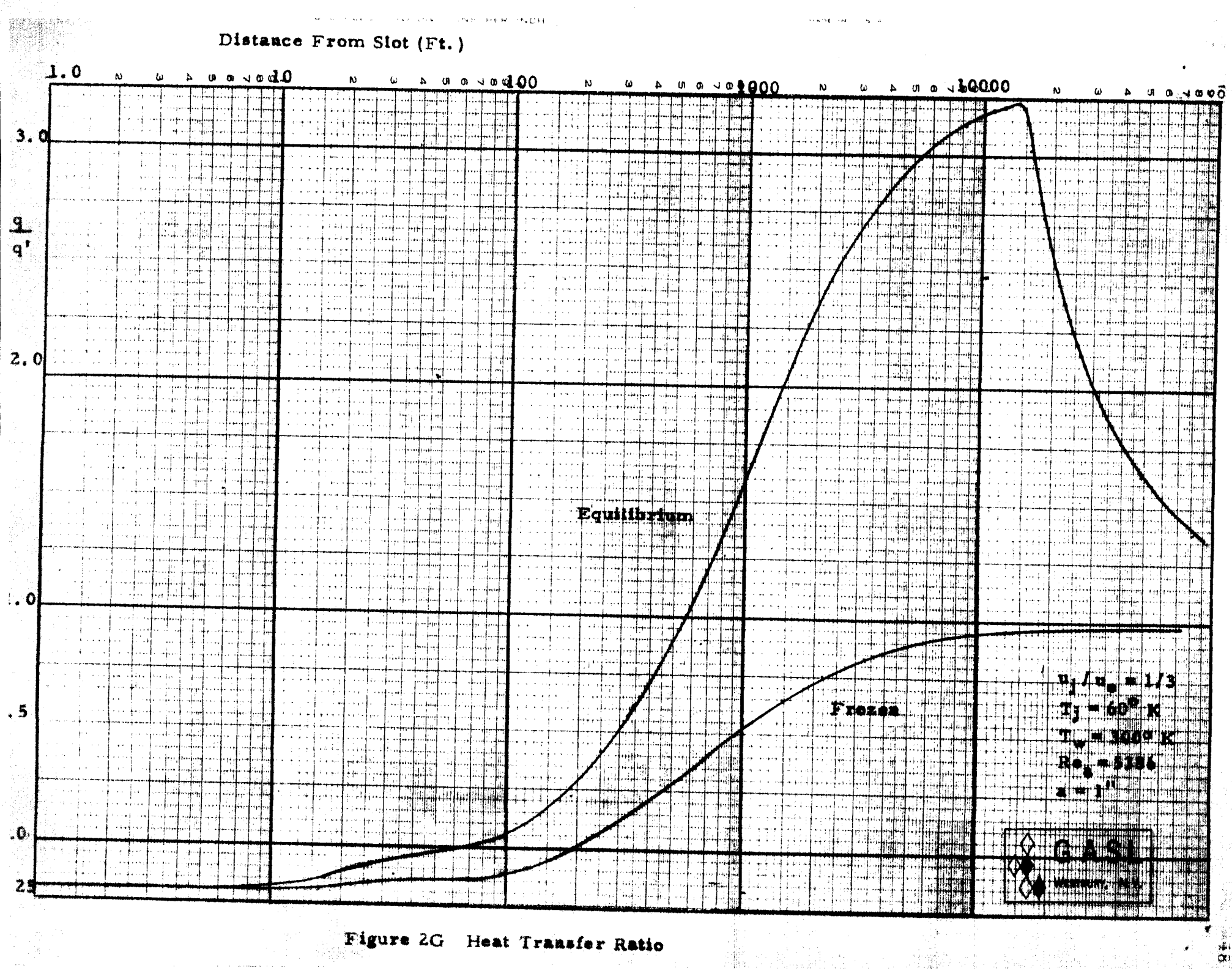

Figure 2G Heat Transfer Ratio

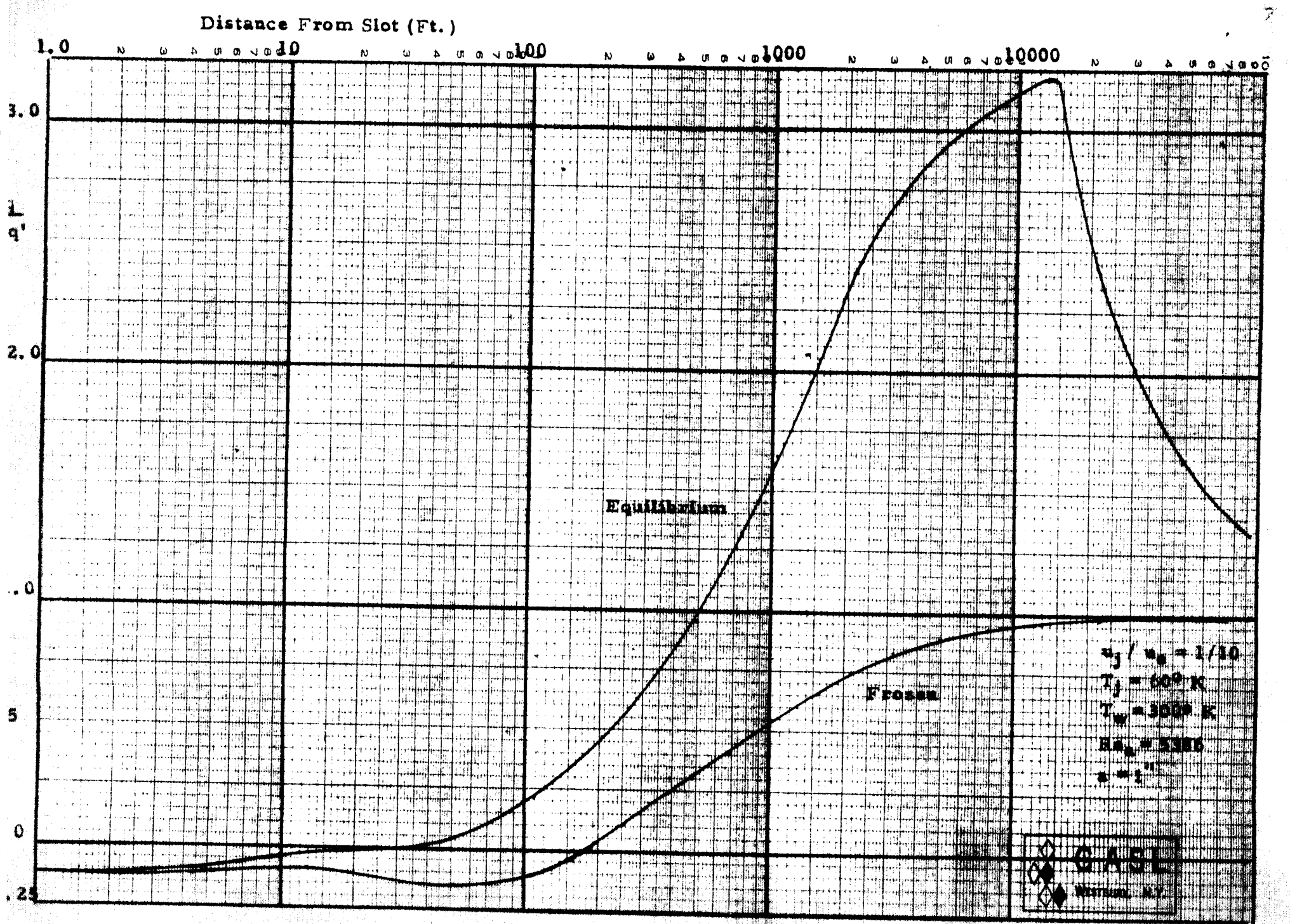

Figure 2H Heat Transfer Ratio

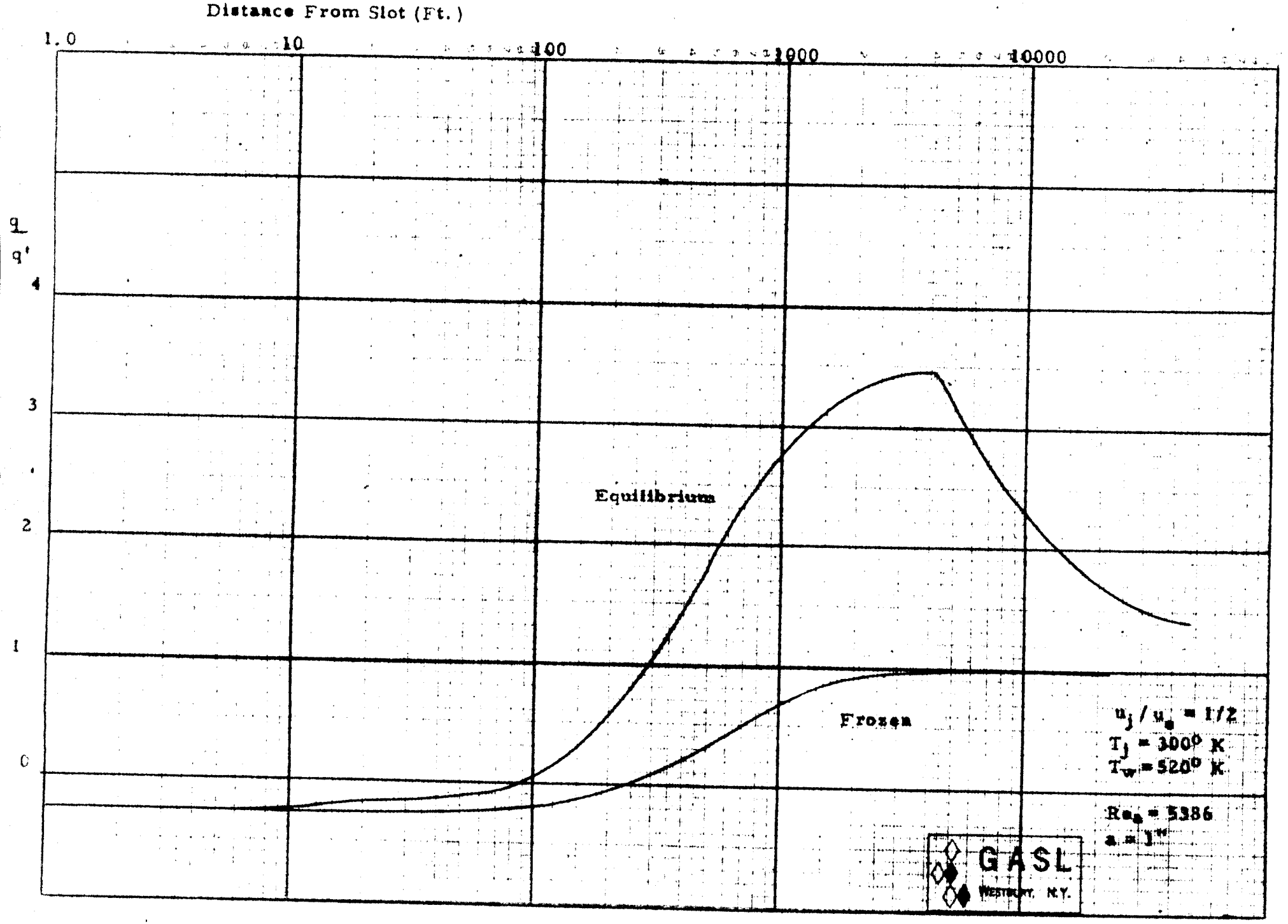

Figure 21 Heat Transfer Ratio

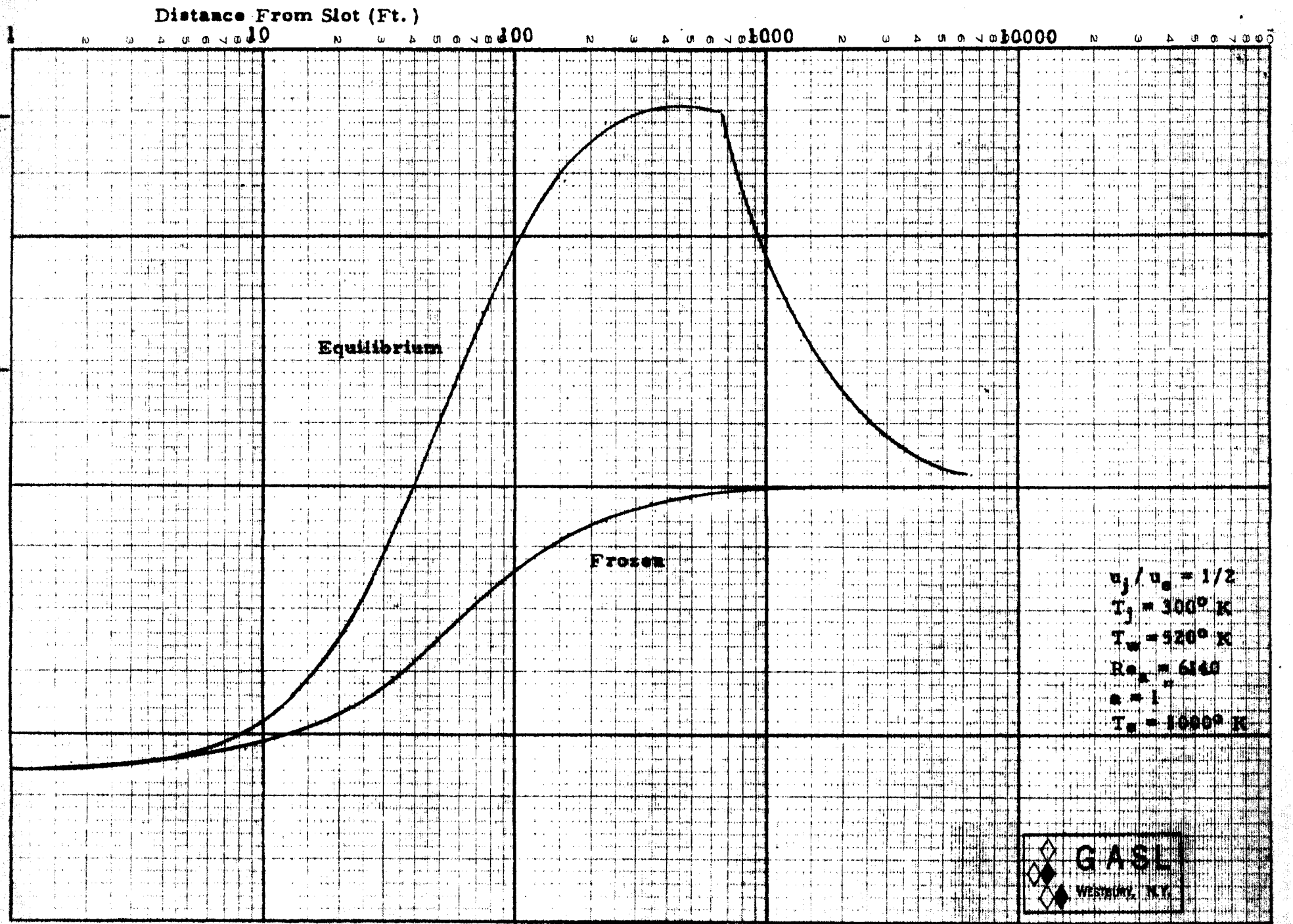

Figure 2J Heat Transfer Ratio

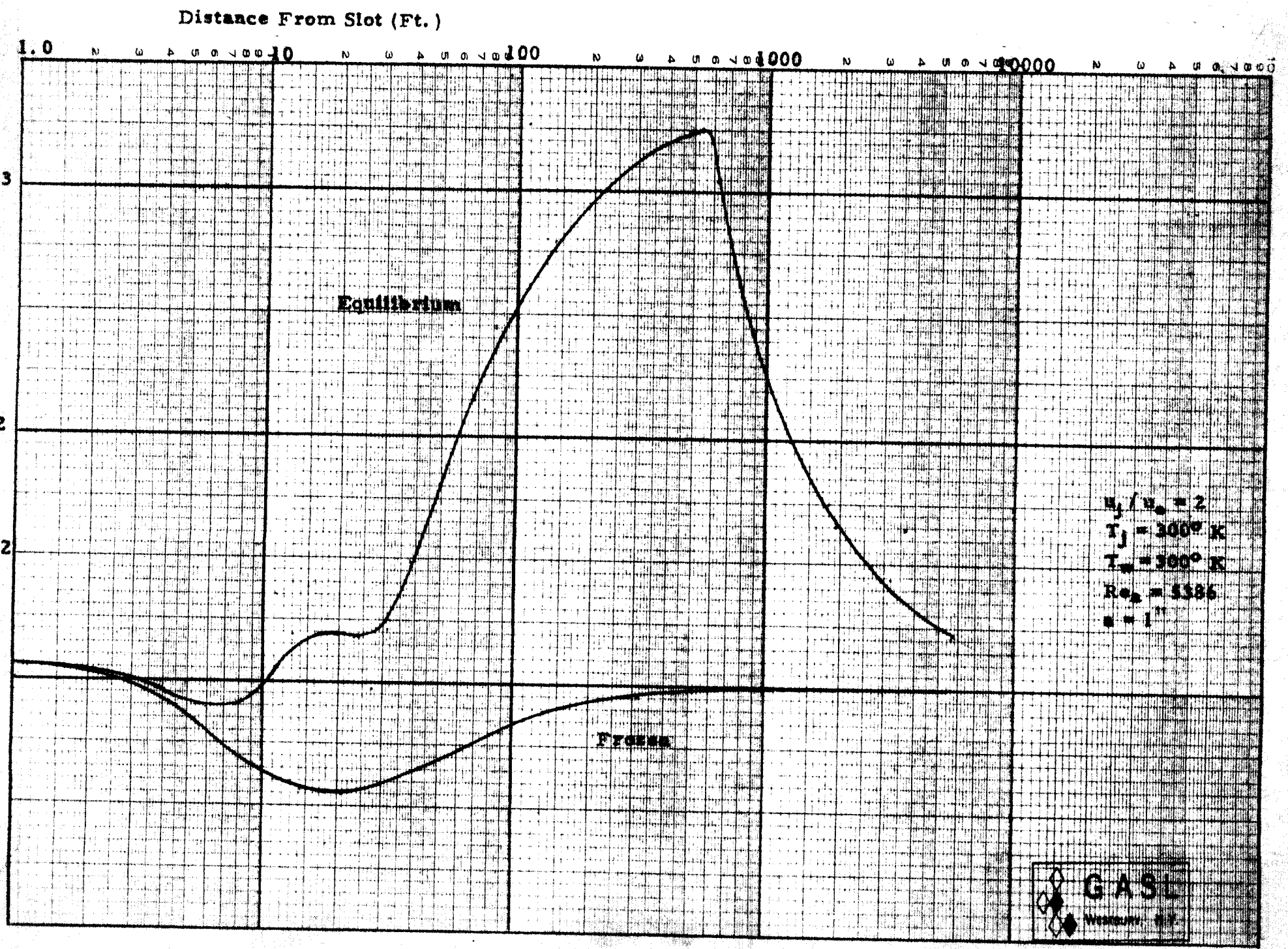

Figure 2K Heat Transfer Ratio

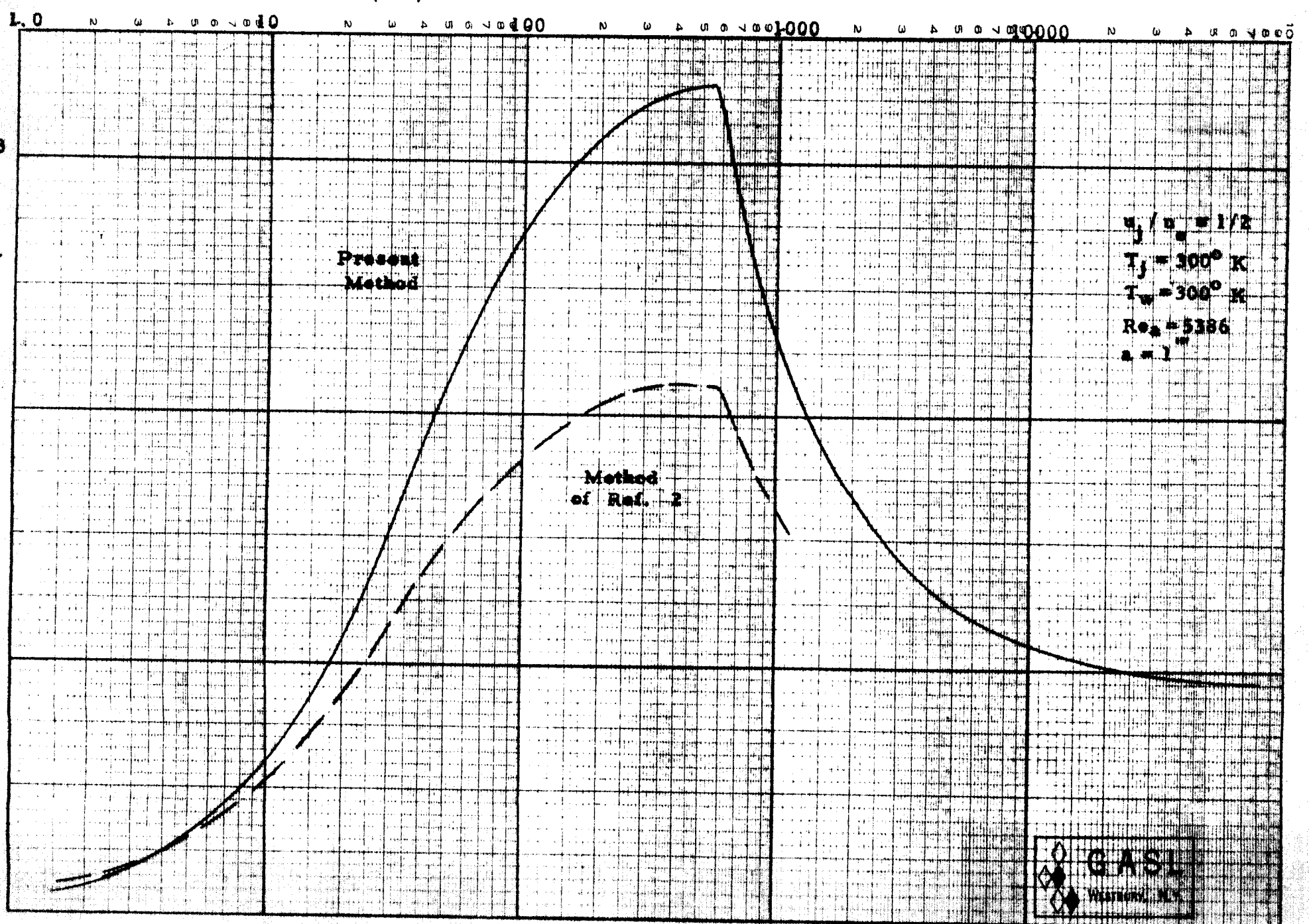

Figure 3 Comparison of Heat Transfer Results (Equilibrium)

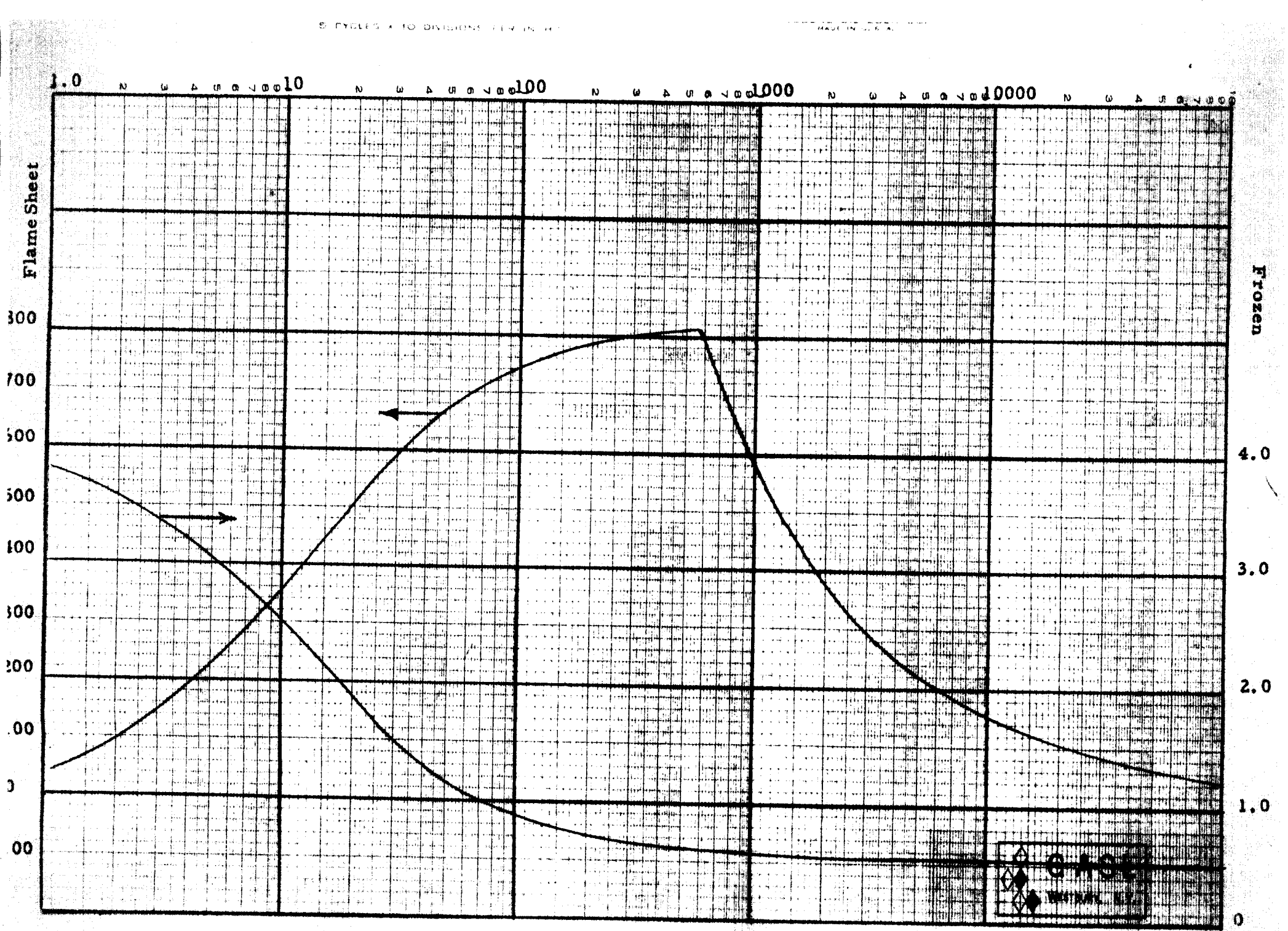

Figure 4 Typical Wall Enthalpy Distributions

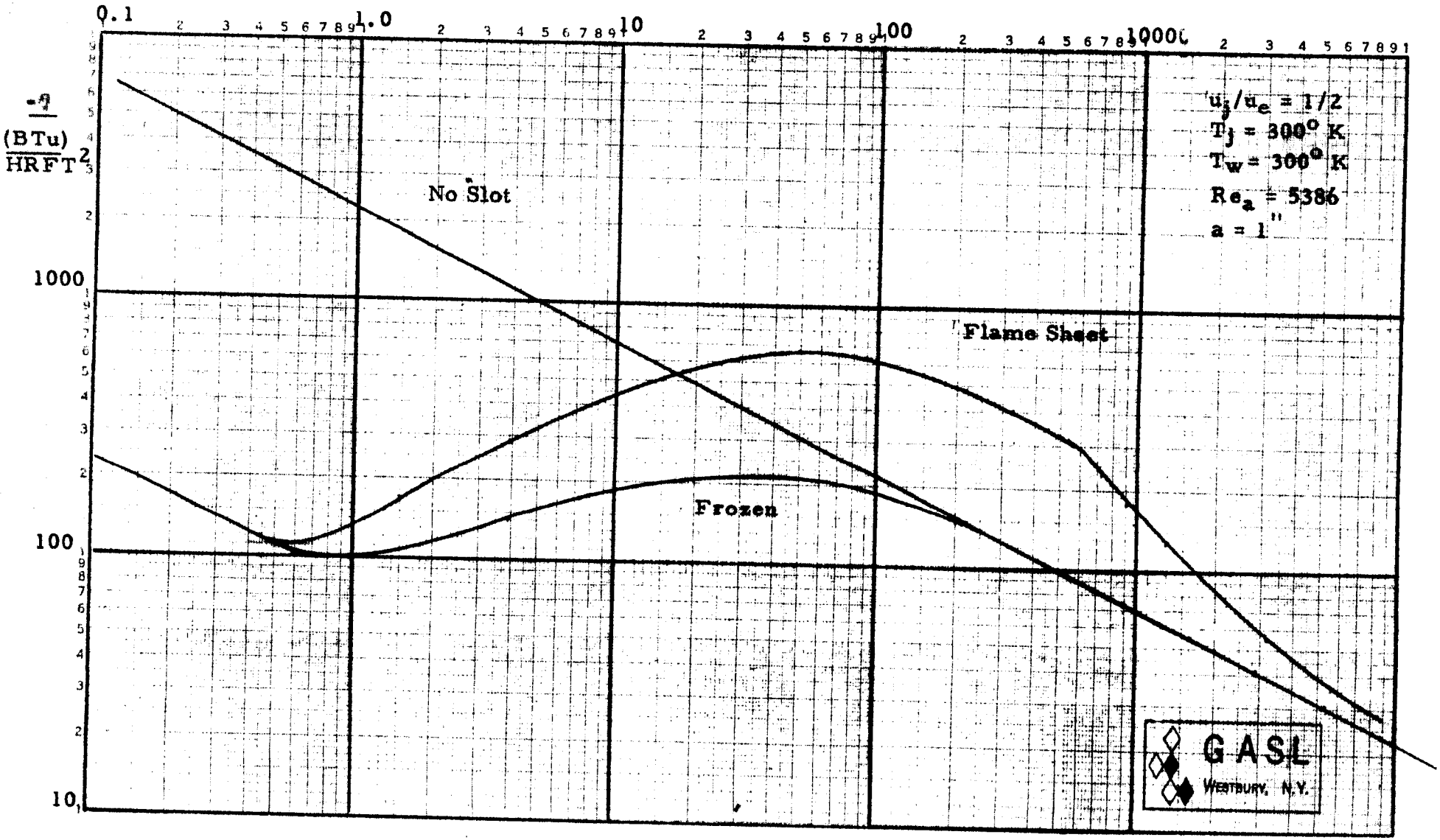

Figure 5 Typical Heat Transfer Distribution

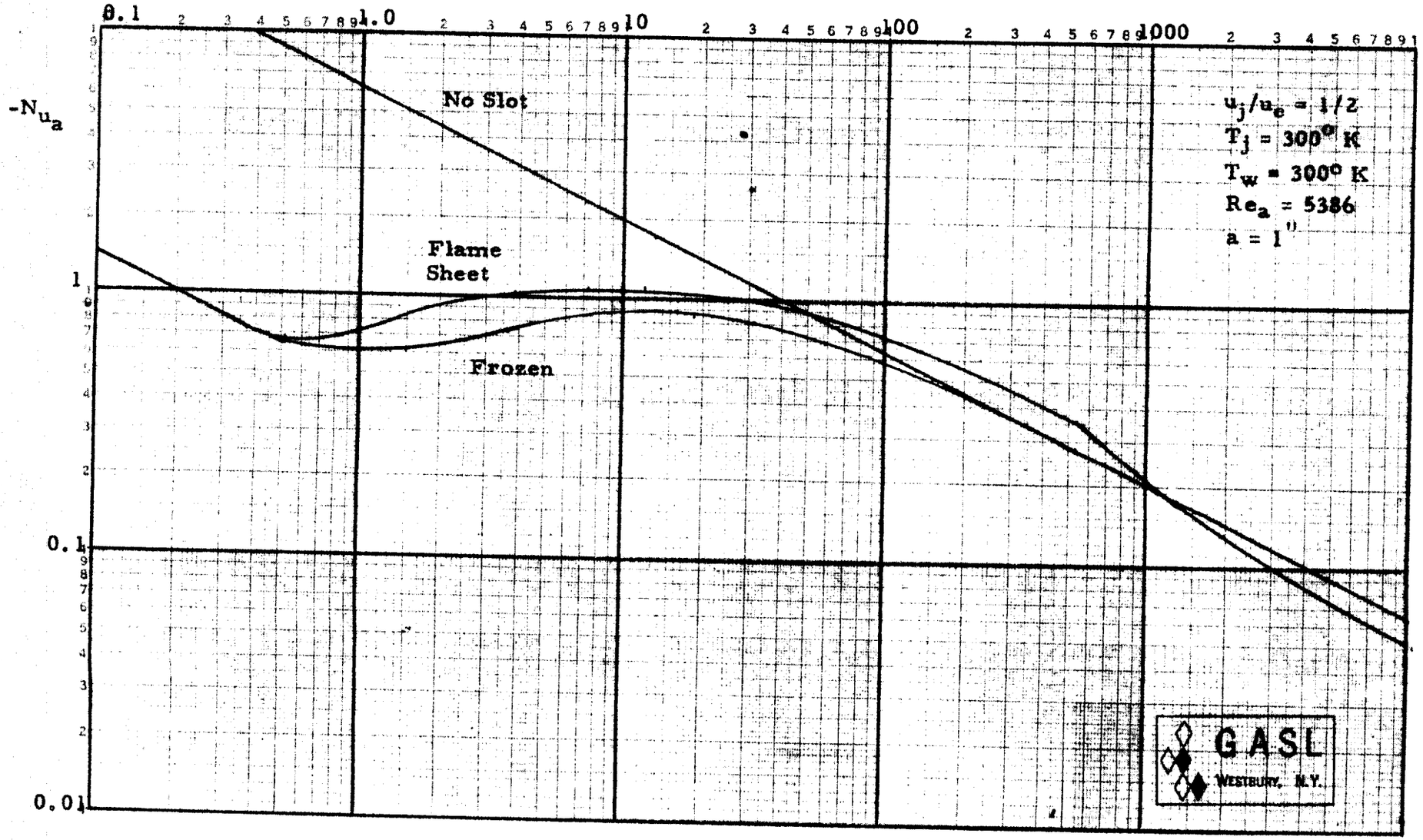

Figure 6 Typical Nusselt Number Distribution

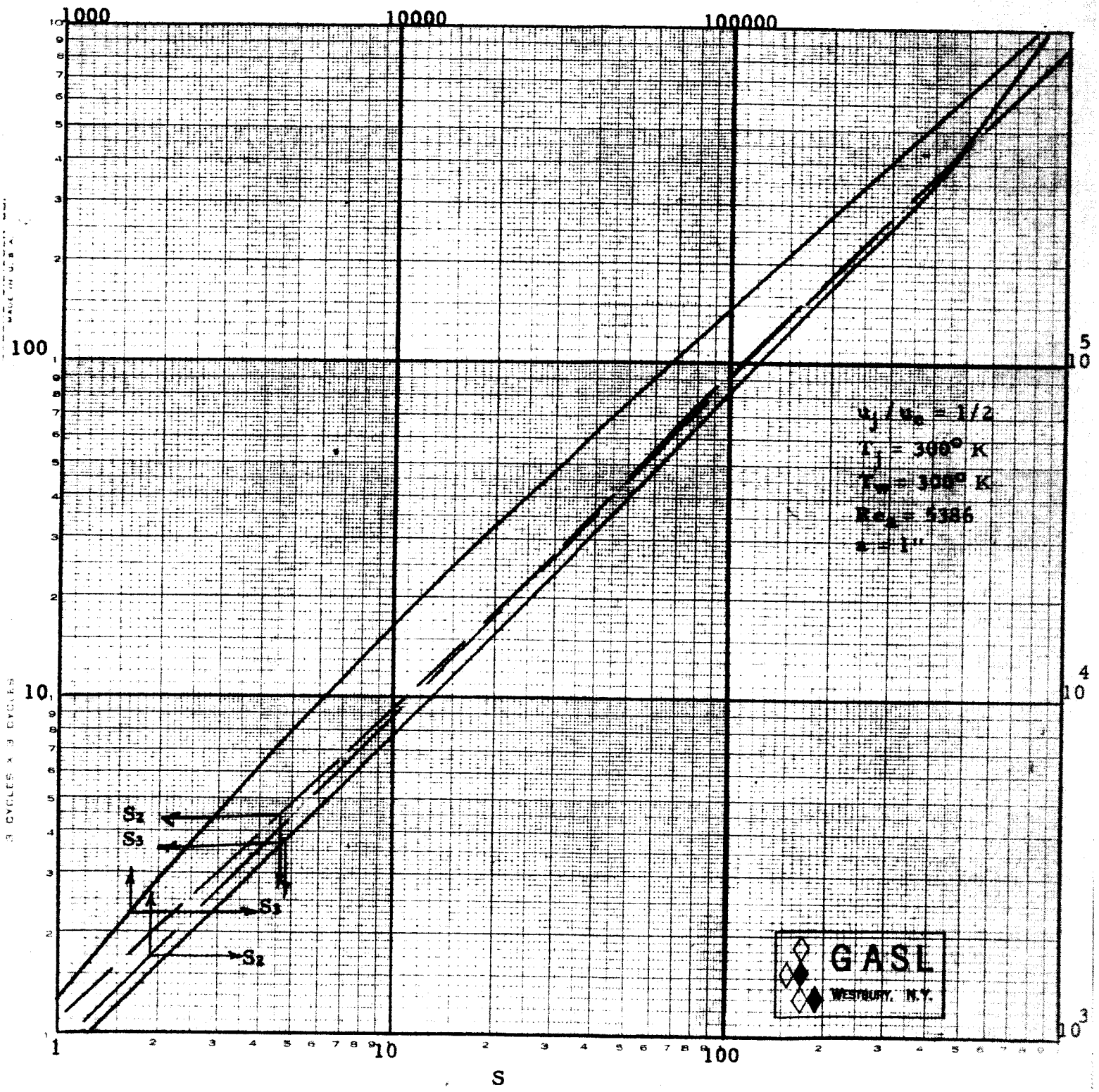

Figure 7A Relation Between Energy, Mass Fraction And Momentum Variables For Equilibrium (Flame Sheet) Chemistry Case

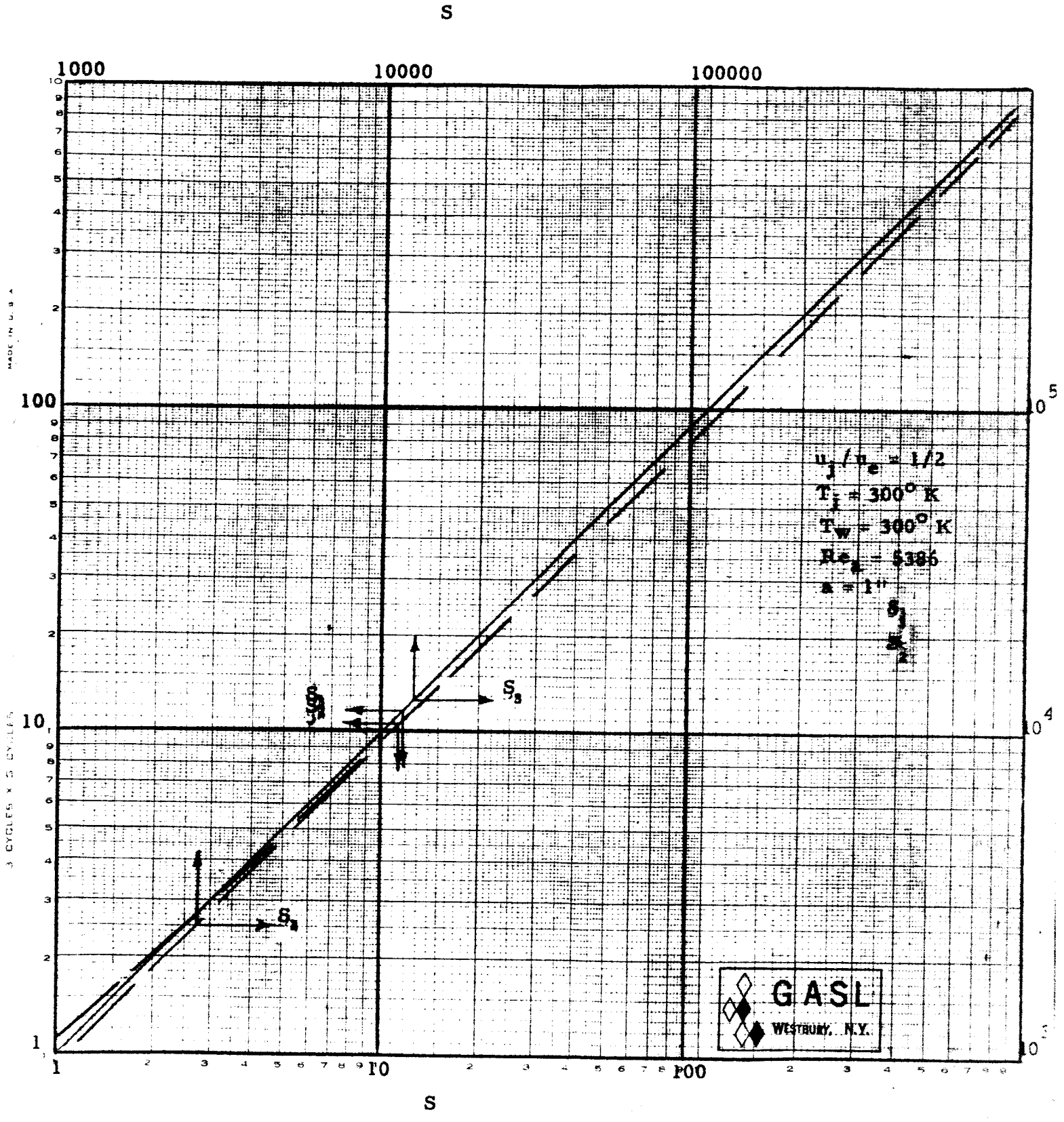

Figure 7B Relation Between Energy, Mass Fraction And Momentum Variables For Frozen Chemistry Case.

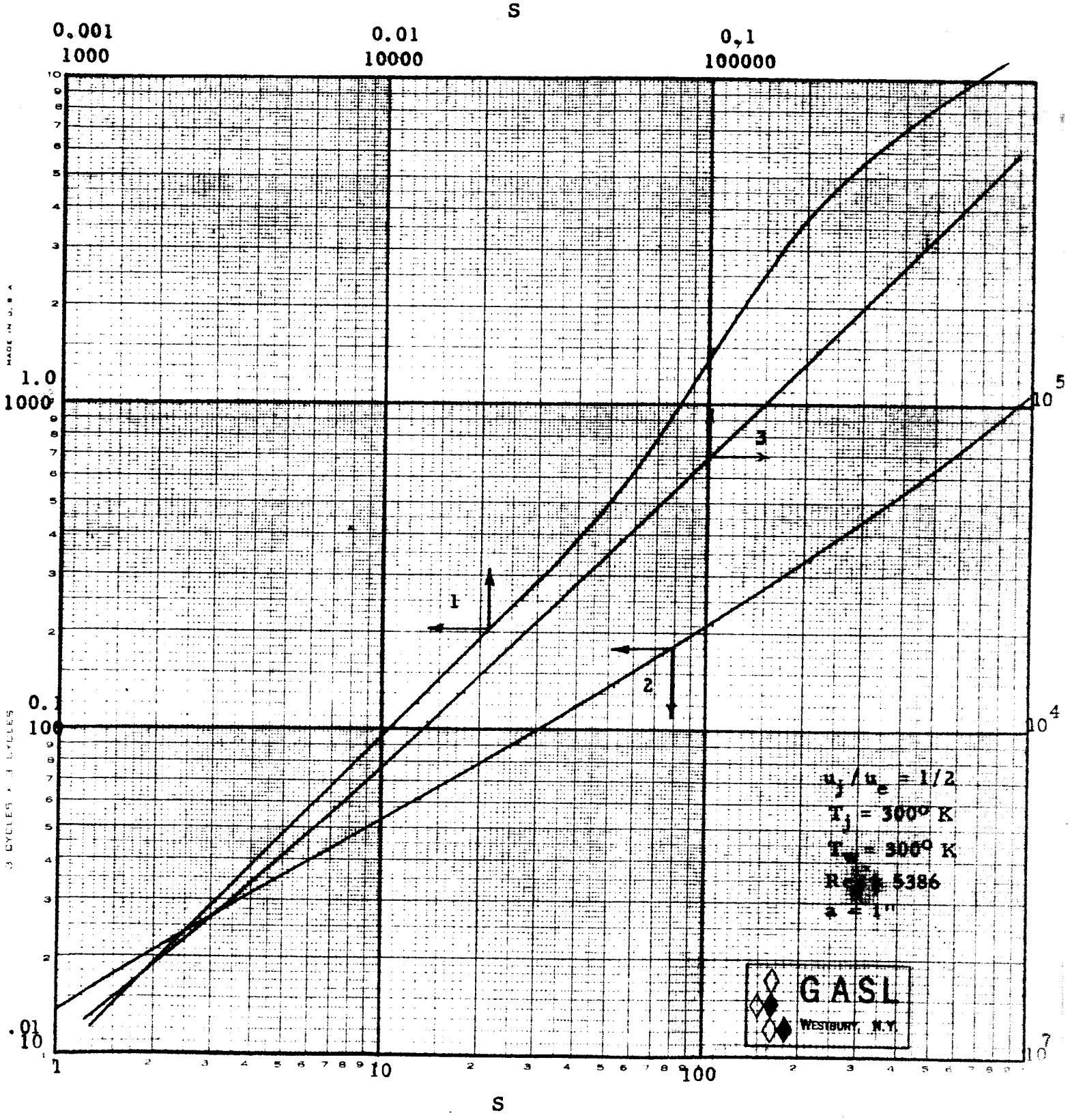

Figure 8A Relation Between Physical and Momentum Coordinates For Equilibrium (Flame Sheet) Chemistry Case

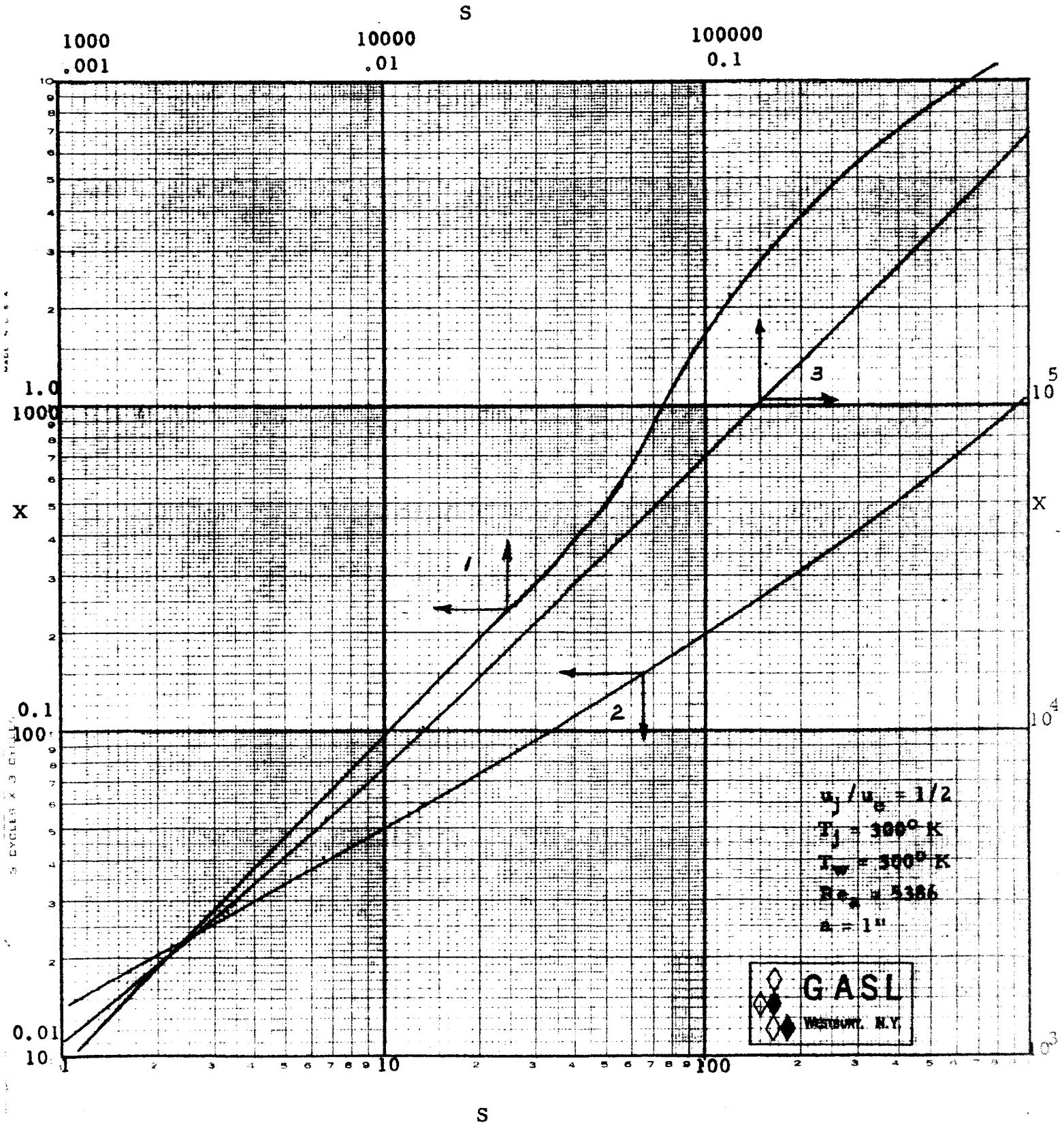

Figure 8B Relation Between Physical and Momentum Coordinates For Frozen Chemistry Case